Measurements of production cross sections of WZ and same-sign WW boson pairs in association with two jets in proton-proton collisions at $\sqrt{s} = 13\,\text{TeV}$

The CMS Collaboration[⋆]

CERN, Switzerland

A B S T R A C T

Measurements of production cross sections of WZ and same-sign WW boson pairs in association with two jets in proton-proton collisions at $\sqrt{s} = 13\,\text{TeV}$ at the LHC are reported. The data sample corresponds to an integrated luminosity of $137\,\text{fb}^{-1}$, collected with the CMS detector during 2016–2018. The measurements are performed in the leptonic decay modes $W^{\pm}Z \to \ell^{\pm}\nu\,\ell'^{\pm}\ell'^{\mp}$ and $W^{\pm}W^{\pm} \to \ell^{\pm}\nu\,\ell'^{\pm}\nu$, where $\ell, \ell' = \text{e}, \mu$. Differential fiducial cross sections as functions of the invariant masses of the jet and charged lepton pairs, as well as of the leading-lepton transverse momentum, are measured for $W^{\pm}W^{\pm}$ production and are consistent with the standard model predictions. The dependence of differential cross sections on the invariant mass of the jet pair is also measured for WZ production. An observation of electroweak production of WZ boson pairs is reported with an observed (expected) significance of 6.8 (5.3) standard deviations. Constraints are obtained on the structure of quartic vector boson interactions in the framework of effective field theory.

© 2020 The Author. Published by Elsevier B.V. This is an open access article under the CC BY license (http://creativecommons.org/licenses/by/4.0/). Funded by SCOAP³.

1. Introduction

The observation of a Higgs boson with a mass of about 125 GeV [1–3] established that the W and Z gauge bosons acquire mass via the Brout–Englert–Higgs mechanism [4–9]. Further insight into the electroweak (EW) symmetry breaking mechanism can be achieved through measurements of vector boson scattering (VBS) processes [10,11]. At the CERN LHC interactions from VBS are characterized by the presence of two gauge bosons, in association with two forward jets with large dijet invariant mass and large rapidity separation, as shown in Fig. 1. They are part of a class of processes contributing to diboson plus two jets production that proceeds via the EW interaction, referred to as EW-induced diboson production, at tree level, $O(\alpha^4)$, where α is the EW coupling. An additional contribution to the diboson states arises via quantum chromodynamics (QCD) radiation of partons from an incoming quark or gluon, leading to tree-level contributions at $O(\alpha^2\alpha_S^2)$, where α_S is the strong coupling. This class of processes is referred to as QCD-induced diboson production.

Modifications of the VBS production cross sections are predicted in models of physics beyond the standard model (SM), for example through changes to the Higgs boson couplings to gauge bosons [10,11]. In addition, the non-Abelian gauge structure of the EW sector of the SM predicts self-interactions between gauge bosons through triple and quartic gauge couplings, which can be probed via measurements of VBS processes [12,13]. The possible presence of anomalous quartic gauge couplings (aQGC) could result in an excess of events with respect to the SM predictions [14].

This letter presents a study of VBS in $W^{\pm}W^{\pm}$ and WZ channels using proton-proton (pp) collisions at $\sqrt{s} = 13\,\text{TeV}$. For the WW measurement, the same-sign $W^{\pm}W^{\pm}$ channel is chosen because of the smaller background yield from SM processes compared to $W^{\pm}W^{\mp}$. The data sample corresponds to an integrated luminosity of $137 \pm 2\,\text{fb}^{-1}$ [15–17] collected with the CMS detector [18] in three separate LHC operating periods during 2016, 2017, and 2018. The three data sets are analyzed independently, with appropriate calibrations and corrections, to account for the various LHC running conditions and the performance of the CMS detector.

The measurements are performed in the leptonic decay modes $W^{\pm}W^{\pm} \to \ell^{\pm}\nu\,\ell'^{\pm}\nu$ and $W^{\pm}Z \to \ell^{\pm}\nu\,\ell'^{\pm}\ell'^{\mp}$, where $\ell, \ell' = \text{e}, \mu$. Fig. 1 shows representative Feynman diagrams involving quartic vertices. Candidate events contain either two identified leptons of the same charge or three identified charged leptons with the total charge of ± 1, moderate missing transverse momentum (p_T^{miss}), and two jets with a large rapidity separation and a large dijet mass.
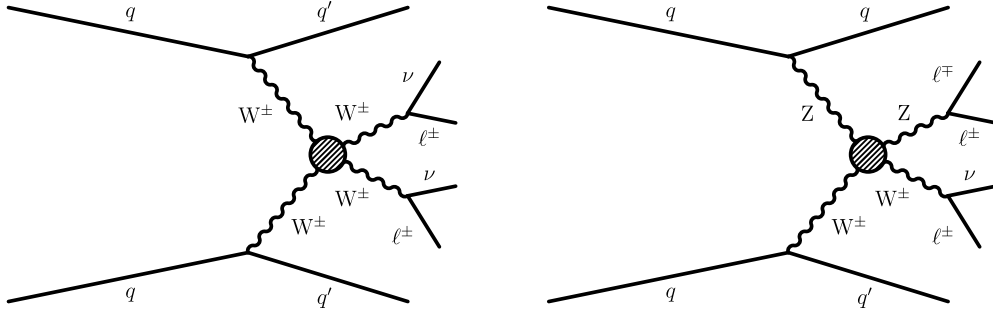
Fig. 1. Representative Feynman diagrams of a VBS process contributing to the EW-induced production of events containing $W^\pm W^\pm$ (left) and WZ (right) boson pairs decaying to leptons, and two forward jets. New physics (represented by a dashed circle) in the EW sector can modify the quartic gauge couplings.
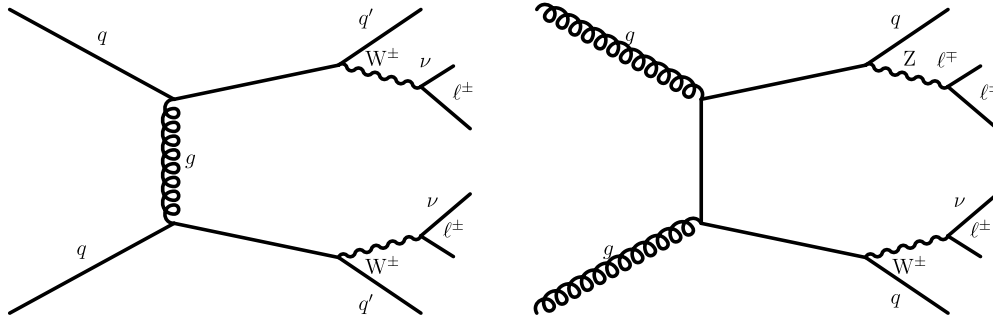

Fig. 2. Representative Feynman diagrams of the QCD-induced production of $W^\pm W^\pm$ (left) and WZ (right) boson pairs decaying to leptons, and two jets.

The requirements on the dijet mass and rapidity separation reduce the contribution from the QCD-induced production of boson pairs in association with two jets, making the experimental signature an ideal topology for VBS studies. Fig. 2 shows representative Feynman diagrams of the QCD-induced production. The EW $W^\pm W^\pm$ and WZ production cross sections are simultaneously measured by performing a binned maximum-likelihood fit of several distributions sensitive to these processes.

The EW production of $W^\pm W^\pm$ at the LHC in the leptonic decay modes has been previously measured at $\sqrt{s} = 8$ and 13 TeV [19–22]. The ATLAS and CMS Collaborations reported observations of the EW $W^\pm W^\pm$ production at 13 TeV with a significance greater than 5 standard deviations using the data collected in 2016, corresponding to integrated luminosities of approximately 36 fb^{-1}. The EW WZ production in the fully leptonic decay modes has been studied at 8 and 13 TeV [23–25]; the ATLAS Collaboration reported an observation at 13 TeV with a significance greater than 5 standard deviations. The EW production of $W^\pm W^\pm$ and WZ boson pairs has also been studied in semileptonic final states [26]. Limits on aQGCs were also reported in Refs. [27,28].

2. The CMS detector

The central feature of the CMS apparatus is a superconducting solenoid of 6 m internal diameter, providing a magnetic field of 3.8 T. Within the solenoid volume are a silicon pixel and strip tracker, a lead-tungstate crystal electromagnetic calorimeter (ECAL), and a brass and scintillator hadron calorimeter, each composed of a barrel and two endcap sections. Forward calorimeters extend the pseudorapidity (η) coverage provided by the barrel and endcap detectors up to $|\eta| < 5$. Muons are detected in gas-ionization chambers embedded in the steel magnetic flux-return yoke outside the solenoid. A more detailed description of the CMS detector, together with a definition of the coordinate system and the relevant kinematic variables, is reported in Ref. [18]. Events of interest are selected using a two-tiered trigger system [29]. The

first level, composed of custom hardware processors, uses information from the calorimeters and muon detectors to select events at a rate of around 100 kHz with a latency of 4 μs. The second level, known as the high-level trigger, consists of a farm of processors running a version of the full event reconstruction software optimized for fast processing, and reduces the event rate to around 1 kHz before data storage.

3. Signal and background simulation

Multiple Monte Carlo (MC) event generators are used to simulate the signal and background contributions. Three sets of simulated events for each process are needed to match the data-taking conditions in the various years.

The SM EW $W^\pm W^\pm$ and WZ processes, where both bosons decay leptonically, are simulated using MadGraph5_amc@nlo 2.4.2 [30–32] at leading order (LO) accuracy with six EW ($O(\alpha^6)$) and zero QCD vertices. MadGraph5_amc@nlo 2.4.2 is also used to simulate the QCD-induced $W^\pm W^\pm$ process. Contributions with an initial-state b quark are excluded from the EW WZ simulation because they are considered part of the tZq background process. Triboson processes, where the WZ boson pair is accompanied by a third vector boson that decays into jets, are included in the simulation. The simulation of the aQGC processes uses the MadGraph5_amc@nlo generator and employs matrix element reweighting to obtain a finely spaced grid of parameters for each of the probed anomalous couplings [33]. The QCD-induced WZ process is simulated at LO with up to three additional partons in the matrix element calculations using the MadGraph5_amc@nlo generator with at least one QCD vertex at tree level. The different jet multiplicities are merged using the MLM scheme [34] to match matrix element and parton shower jets, and the inclusive contribution is normalized to next-to-next-to-leading order (NNLO) predictions [35]. The interference between the EW and QCD diagrams is also produced with MadGraph5_amc@nlo. The contribution of the interference is considered to be part of the EW

production, leading to an increase of about 4 and 1% of the expected yields of the EW $W^{\pm}W^{\pm}$ and WZ processes in the fiducial region, respectively.

A complete set of next-to-leading order (NLO) QCD and EW corrections for the leptonic $W^{\pm}W^{\pm}$ scattering process have been computed [36,37] and they reduce the LO cross section of the EW $W^{\pm}W^{\pm}$ process at the level of 10-15%, with the correction increasing in magnitude with increasing dilepton and dijet invariant masses. Similarly, the NLO QCD and EW corrections for the leptonic WZ scattering process have been computed at the orders of $O(\alpha_S\alpha^6)$ and $O(\alpha^7)$ [38], reducing the cross sections for the EW WZ process at the level of 10%. The predictions for the cross sections of the EW $W^{\pm}W^{\pm}$ and WZ processes are also made after applying these $O(\alpha_S\alpha^6)$ and $O(\alpha^7)$ corrections to MAD-GRAPH5_aMC@NLO LO cross sections. These corrections have approximately 1% effect on the measurements and are not included at the data analysis level. Satisfactory agreement between predictions from MADGRAPH5_aMC@NLO and various event generators and fixed-order calculations in the fiducial region is reported in Ref. [39].

The POWHEG v2 [40–44] generator is used to simulate the $t\bar{t}$, tW, and other diboson processes at NLO accuracy in QCD. Production of $t\bar{t}W$, $t\bar{t}Z$, $t\bar{t}\gamma$, and triple vector boson (VVV) background events is simulated at NLO accuracy in QCD using the MAD-GRAPH5_aMC@NLO 2.2.2 (2.4.2) generator [30–32] for 2016 (2017 and 2018) samples. The tZq process is simulated at NLO in the four-flavor scheme using MADGRAPH5_aMC@NLO 2.3.3. The MC simulation is normalized using a cross section computed at NLO with MADGRAPH5_aMC@NLO in the five-flavor scheme, following the procedure of Ref. [45]. The double parton scattering $W^{\pm}W^{\pm}$ production is generated at LO using PYTHIA 8.226 (8.230) [46] in 2016 (2017 and 2018).

The NNPDF 3.0 NLO [47] (NNPDF 3.1 NNLO [48]) parton distribution functions (PDFs) are used for simulating all 2016 (2017 and 2018) samples. For all processes, the parton showering and hadronization are simulated using PYTHIA 8.226 (8.230) in 2016 (2017 and 2018). The modeling of the underlying event is generated using the CUETP8M1 [49,50] (CP5 [51]) tune for simulated samples corresponding to the 2016 (2017 and 2018) data.

All MC generated events are processed through a simulation of the CMS detector based on GEANT4 [52] and are reconstructed with the same algorithms used for data. Additional pp interactions in the same and nearby bunch crossings, referred to as pileup, are also simulated. The distribution of the number of pileup interactions in the simulation is adjusted to match the one observed in the data. The average number of pileup interactions was 23 (32) in 2016 (2017 and 2018).

4. Event reconstruction

The CMS particle-flow (PF) algorithm [53] is used to combine the information from all subdetectors for particle reconstruction and identification. The vector $\vec{p}_T^{\text{miss}}$ is defined as the projection onto the plane perpendicular to the beam axis of the negative vector momentum sum of all reconstructed PF objects in an event. Its magnitude is referred to as p_T^{miss}.

Jets are reconstructed by clustering PF candidates using the anti-k_T algorithm [54] with a distance parameter R = 0.4. Jets are calibrated in the simulation, and separately in data, accounting for energy deposits of neutral particles from pileup and any non-linear detector response [55,56]. Jets with transverse momentum $p_T > 50$ GeV and $|\eta| < 4.7$ are included in the analysis. The effect of pileup is mitigated through a charged-hadron subtraction technique, which removes the energy of charged hadrons not originating from the event primary vertex (PV) [57]. Jet energy corrections

to the detector measurements are propagated to p_T^{miss} [58]. The PV is defined as the vertex with the largest value of summed physics-object p_T^2. Here, the physics objects are the jets clustered using the jet finding algorithm [54,59] with the tracks assigned to the vertex as inputs, and the associated p_T^{miss}, taken as the negative vector p_T sum of those jets.

The DEEPCSV b tagging algorithm [60] is used to identify events containing a jet that is consistent with the fragmentation of a bottom quark. This tagging algorithm, an improved version of previous taggers, was developed using a deep neural network with a more sophisticated architecture and it provides a simultaneous training in both secondary vertex categories and jet flavors. For the chosen working point, the efficiency to select b quark jets is about 72% and the rate for incorrectly tagging jets originating from the hadronization of gluons or u, d, s quarks is about 1%.

Electrons and muons are reconstructed by associating a track reconstructed in the tracking detectors with either a cluster of energy in the ECAL [61] or a track in the muon system [62]. Electrons (muons) must pass "loose" identification criteria with $p_T > 10$ GeV and $|\eta| < 2.5$ (2.4) to be selected for the analysis. At the final stage of the lepton selection, tight working points, following the definitions provided in Refs. [61,62], are chosen for the identification criteria, including requirements on the impact parameter of the candidates with respect to the PV and their isolation with respect to other particles in the event [63]. For electrons, the background contribution coming from a mismeasurement of the track charge is not negligible. The sign of this charge is evaluated with three different observables that measure the electron curvature using different methods; requiring all three charge evaluations to agree reduces this background contribution by a factor of five with an efficiency of about 97% [61]. For muons, the charge mismeasurement is negligible [64,65].

5. Event selection

Collision events are collected using single-electron and single-muon triggers that require the presence of an isolated lepton with p_T larger than 27 and 24 GeV, respectively. In addition, a set of dilepton triggers with lower p_T thresholds are used, ensuring a trigger efficiency above 99% for events that satisfy the subsequent offline selection.

Several selection requirements are used to isolate the VBS topology by reducing the contributions from background processes. By inverting some of these selection requirements we can select background-enriched control regions (CRs). In the offline analysis, events with two or three isolated charged leptons with $p_T > 10$ GeV and at least two jets with $p_T^j > 50$ GeV and $|\eta| < 4.7$ are accepted as candidate events. Jets that are within $\Delta R = \sqrt{(\Delta\eta)^2 + (\Delta\phi)^2} < 0.4$ of one of the identified charged leptons are excluded. Candidate events with four or more charged leptons satisfying the loose identification criteria are rejected.

In the WZ candidate events, one of the oppositely charged same-flavor leptons from the Z boson candidate is required to have $p_T > 25$ GeV and the other $p_T > 10$ GeV with the invariant mass of the dilepton pair $m_{\ell\ell}$ satisfying $|m_{\ell\ell} - m_Z| < 15$ GeV. In candidate events with three same-flavor leptons, the oppositely charged lepton pair with the invariant mass closest to the nominal Z boson mass m_Z [66] is selected as the Z boson candidate. The third lepton with $p_T > 20$ GeV is associated with the W boson. In addition, the trilepton invariant mass $m_{\ell\ell\ell}$ is required to exceed 100 GeV.

One of the leptons in the same-sign $W^{\pm}W^{\pm}$ candidate events is required to have $p_T > 25$ GeV and the other $p_T > 20$ GeV. The invariant mass of the dilepton pair $m_{\ell\ell}$ must be greater than 20 GeV. Candidate events in the dielectron final state with $|m_{\ell\ell} - m_Z| < 15$ GeV are rejected to reduce the number of Z boson background

Table 1

Summary of the selection requirements defining the $W^{\pm}W^{\pm}$ and WZ SRs. The looser lepton p_T requirement on the WZ selection refers to the trailing lepton from the Z boson decays. The $|m_{\ell\ell} - m_Z|$ requirement is applied to the dielectron final state only in the $W^{\pm}W^{\pm}$ SR.

Variable	$W^{\pm}W^{\pm}$	WZ
Leptons	2 leptons, $p_T > 25/20\,\text{GeV}$	3 leptons, $p_T > 25/10/20\,\text{GeV}$
p_T^j	$>50\,\text{GeV}$	$>50\,\text{GeV}$
$\lvert m_{\ell\ell} - m_Z \rvert$	$>15\,\text{GeV}$ (ee)	$<15\,\text{GeV}$
$m_{\ell\ell}$	$>20\,\text{GeV}$	–
$m_{\ell\ell\ell}$	–	$>100\,\text{GeV}$
p_T^{miss}	$>30\,\text{GeV}$	$>30\,\text{GeV}$
b quark veto	Required	Required
$\max(z_\ell^*)$	<0.75	<1.0
m_{jj}	$>500\,\text{GeV}$	$>500\,\text{GeV}$
$\lvert \Delta\eta_{jj} \rvert$	>2.5	>2.5

events where the charge of one of the electron candidates is misidentified.

The VBS topology is targeted by requiring a large dijet invariant mass $m_{jj} > 500\,\text{GeV}$ and a large pseudorapidity separation $|\Delta\eta_{jj}| > 2.5$. The candidate $W^{\pm}W^{\pm}$ (WZ) events are also required to have $\max(z_\ell^*) < 0.75$ (1.0), where

$$z_\ell^* = \left| \eta^\ell - \frac{\eta^{j_1} + \eta^{j_2}}{2} \right| / |\Delta\eta_{jj}| \qquad (1)$$

is the Zeppenfeld variable [67], η^ℓ is the pseudorapidity of a lepton, and η^{j_1} and η^{j_2} are the pseudorapidities of the two candidate VBS jets. In the case of more than two jet candidates, the two jets with the largest p_T are selected.

The p_T^{miss} associated with the undetected neutrinos is required to be greater than 30 GeV. The list of selection requirements used to define the same-sign $W^{\pm}W^{\pm}$ and WZ signal regions (SRs) is summarized in Table 1. The $W^{\pm}W^{\pm}$ SR is dominated by the EW signal process, whereas the WZ SR has a very large component of the QCD WZ process, as seen in Table 4.

6. Background estimation

A combination of methods based on CRs in data and simulation is used to estimate background contributions. Uncertainties related to the theoretical and experimental predictions are estimated as described in Section 7. The normalization of the WZ contribution in the $W^{\pm}W^{\pm}$ SR is constrained by the data in the WZ SR, which is evaluated simultaneously for the extraction of results. The background contribution from charge misidentification (wrong-sign) is estimated by applying a data-to-simulation efficiency correction due to charge-misidentified electrons. The electron charge misidentification rate, estimated using Drell–Yan events, is about 0.01 (0.3)% in the barrel (endcap) region [61,68].

The nonprompt lepton backgrounds originating from leptonic decays of heavy quarks, hadrons misidentified as leptons, and electrons from photon conversions are suppressed by the identification and isolation requirements imposed on electrons and muons. The remaining contribution from the nonprompt lepton background is estimated directly from a data sample following the technique described in Ref. [19]. This sample is selected by choosing events using the final selection criteria, except for one of the leptons for which the selection is relaxed to a looser criteria and that has failed the nominal selection. The yield in this sample is extrapolated to the signal region using the efficiencies for such loosely identified leptons to pass the standard lepton selection criteria. This efficiency is calculated in a sample of events dominated by dijet production. A normalization uncertainty of 20% is assigned

for the nonprompt lepton background to include possible differences in the composition of jets between the data sample used to derive these efficiencies and the data samples in the $W^{\pm}W^{\pm}$ and WZ SRs [63].

Three CRs are used to select nonprompt lepton, tZq, and ZZ background-enriched events to further estimate these processes from data. The ZZ process is treated as background since the analysis selection is not sensitive to the EW ZZ production. The nonprompt lepton CR is defined by requiring the same selection as for the $W^{\pm}W^{\pm}$ SR, but with the b quark veto requirement inverted. The selected events are enriched with the nonprompt lepton background, coming mostly from semileptonic $t\bar{t}$ events, and further estimates the contribution of this background process in the $W^{\pm}W^{\pm}$ SR. Similarly, the tZq CR is defined by requiring the same selection as for the WZ SR, but with the b quark veto requirement inverted. The selected events are dominated by the tZq background process. Finally, the ZZ CR selects events with four leptons with the same VBS-like requirements. The three CRs are used to estimate the normalization of the main background processes from data. All other background processes are estimated from simulation after applying corrections to account for small differences between data and simulation.

Two sets of additional CRs are defined for the $W^{\pm}W^{\pm}$ and WZ measurements to validate the predictions of the background processes. The first CR is defined by requiring the same selection as for the $W^{\pm}W^{\pm}$ SR, but with a requirement of $200 < m_{jj} < 500\,\text{GeV}$. The second CR is defined by selecting events satisfying the requirements on the leptons, p_T^j, and m_{jj}, but with at least one of the other requirements in Table 1 not satisfied. Good agreement between the data and predicted yields is observed in all these regions.

7. Systematic uncertainties

Multiple sources of systematic uncertainty are estimated for these measurements. Independent sources of uncertainty are treated as uncorrelated. The impact in different bins of a differential distribution is considered fully correlated for each source of uncertainty.

The uncertainties in the integrated luminosity measurements for the data used in this analysis are 2.5, 2.3, and 2.5% for the 2016, 2017, and 2018 data samples [15–17], respectively. They are treated as uncorrelated across the three data sets.

The simulation of pileup events assumes a total inelastic pp cross section of 69.2 mb, with an associated uncertainty of 5% [69, 70], which has an impact on the expected signal and background yields of about 1%.

Discrepancies in the lepton reconstruction and identification efficiencies between data and simulation are corrected by applying scale factors to all simulation samples. These scale factors, which depend on the p_T and η for both electrons and muons, are determined using $Z \to \ell\ell$ events in the Z boson peak region that were recorded with independent triggers [61,62,71]. The uncertainty in the determination of the trigger efficiency leads to an uncertainty smaller than 1% in the expected signal yield. The lepton momentum scale uncertainty is computed by varying the momenta of the leptons in simulation by their uncertainties, and repeating the analysis selection. The resulting uncertainties in the yields are $\approx 1\%$ for both electrons and muons. These uncertainties are treated as correlated across the three data sets.

The uncertainty in the calibration of the jet energy scale (JES) directly affects the acceptance of the jet multiplicity requirement and the p_T^{miss} measurement. These effects are estimated by shifting the JES in the simulation up and down by one standard deviation. The uncertainty in the JES is 2–5%, depending on p_T and η [55,56], and the impact on the expected signal and background

Table 2
Relative systematic uncertainties in the EW $W^{\pm}W^{\pm}$ and WZ cross section measurements in units of percent.

Source of uncertainty	$W^{\pm}W^{\pm}$ (%)	WZ (%)
Integrated luminosity	1.5	1.6
Lepton measurement	1.8	2.9
Jet energy scale and resolution	1.5	4.3
Pileup	0.1	0.4
b tagging	1.0	1.0
Nonprompt rate	3.5	1.4
Trigger	1.1	1.1
Limited sample size	2.6	3.7
Theory	1.9	3.8
Total systematic uncertainty	5.7	7.9
Statistical uncertainty	8.9	22
Total uncertainty	11	23

yields is about 3%. There is a larger JES uncertainty in the EW WZ cross section measurement since a multivariate analysis is used for the measurement, which helps discriminate against the background processes, but also increases the corresponding uncertainty, as seen in Table 2.

The b tagging efficiency in the simulation is corrected using scale factors determined from data [60]. These values are estimated separately for correctly and incorrectly identified jets. Each set of values results in uncertainties in the b tagging efficiency of about 1–4%, and the impact on the expected signal and background yields is about 1%. The uncertainties in the JES and b tagging are treated as uncorrelated across the three data sets.

Because of the choice of the QCD renormalization and factorization scales, the theoretical uncertainties are estimated by varying these scales independently up and down by a factor of two from their nominal values (excluding the two extreme variations) and taking the largest cross section variations as the uncertainty [39]. The PDF uncertainties are evaluated according to the procedure described in Ref. [72]. The statistical uncertainties that are associated with the limited number of simulated events and data events used to estimate the nonprompt lepton background are also considered as systematic uncertainties; the data events are the dominant contribution.

A summary of the relative systematic uncertainties in the EW $W^{\pm}W^{\pm}$ and WZ cross sections is shown in Table 2. The slightly larger theoretical uncertainty in the EW WZ cross section measurement arises from the difficulty of disentangling the EW and QCD components in the discriminant fit.

8. Results

To discriminate between the signals and the remaining backgrounds, a binned maximum-likelihood fit is performed using the $W^{\pm}W^{\pm}$ and WZ SRs, and the nonprompt lepton, tZq, and ZZ CRs. The normalization factors for the tZq and ZZ background processes are included in the maximum-likelihood fit together with the EW $W^{\pm}W^{\pm}$, EW WZ, and QCD WZ signal cross sections. The QCD $W^{\pm}W^{\pm}$ contribution is small and is taken from the SM prediction. The systematic uncertainties are treated as nuisance parameters in the fit [73,74].

The value of m_{jj} is effective in discriminating between the signal and background processes because VBS topologies typically exhibit large values for the dijet mass. The value of $m_{\ell\ell}$ is also effective in discriminating between signal and background processes because the nonprompt lepton processes tend to have rather small $m_{\ell\ell}$ values. A two-dimensional distribution is used in the fit for the $W^{\pm}W^{\pm}$ SR with 8 bins in m_{jj} ([500, 650, 800, 1000, 1200, 1500, 1800, 2300, ∞] GeV) and 4 bins in $m_{\ell\ell}$ ([20, 80, 140, 240, ∞] GeV).

A boosted decision tree (BDT) is trained using the TMVA package [75] with gradient boosting and optimized on simulated events

to better separate the EW WZ and QCD WZ processes in the WZ SR by exploring the kinematic differences. Several discriminating observables are used as the BDT inputs, including the jet and lepton kinematics and p_T^{miss}, as listed in Table 3. A larger set of discriminating observables was studied, but only variables improving the sensitivity and showing some signal-to-background separation are retained. The BDT score distribution is used for the WZ SR in the fit with 8 bins ([-1, -0.28, 0.0, 0.23, 0.43, 0.60, 0.74, 0.86, 1]). The m_{jj} distribution is used for the CRs in the fit with 4 bins ([500, 800, 1200, 1800, ∞] GeV). The bin boundaries are chosen to have the same EW $W^{\pm}W^{\pm}$ and WZ contributions across the bins as expected from simulation.

The distributions of m_{jj} and $m_{\ell\ell}$ in the $W^{\pm}W^{\pm}$ SR, and the distributions of m_{jj} and BDT score in the WZ SR are shown in Fig. 3. The data yields, together with the numbers of fitted signal and background events, are given in Table 4. The table also shows the result of a fit to the Asimov data set [76]. The significance of the EW WZ signal is quantified from the p-value using a profile ratio test statistic [73,74] and asymptotic results for the test statistic [76]. The observed (expected) statistical significance of the EW WZ signal is 6.8 (5.3) standard deviations, while the statistical significance of the EW $W^{\pm}W^{\pm}$ signal is far above 5 standard deviations.

8.1. Inclusive and differential fiducial cross section measurements

The fiducial region is defined by a common set of kinematic requirements in the muon and electron final states at the generator level, emulating the selection performed at the reconstruction level. The measured distributions, after subtracting the contributions from the background processes, are corrected for detector resolution effects and inefficiencies. The leptons at generator level are selected at the so-called dressed level by combining the four-momentum of each lepton after the final-state photon radiation with that of photons found within a cone of $\Delta R = 0.1$ around the lepton. The $W^{\pm}W^{\pm}$ fiducial region is defined by requiring two same-sign leptons with $p_T > 20$ GeV, $|\eta| < 2.5$, and $m_{\ell\ell} > 20$ GeV, and two jets with $m_{jj} > 500$ GeV and $|\Delta\eta_{jj}| > 2.5$. The jets at generator level are clustered from stable particles, excluding neutrinos, using the anti-k_T clustering algorithm with R = 0.4, and are required to have $p_T > 50$ GeV and $|\eta| < 4.7$. The jets within $\Delta R < 0.4$ of the selected charged leptons are not included. The WZ fiducial region is defined by requiring three leptons with $p_T > 20$ GeV, $|\eta| < 2.5$, a pair of opposite charge same-flavor lepton pair with $|m_{\ell\ell} - m_Z| < 15$ GeV, and two jets with $m_{jj} > 500$ GeV and $|\Delta\eta_{jj}| > 2.5$. MADGRAPH5_aMC@NLO is used to extrapolate from the reconstruction level to the fiducial phase space. Electrons and muons produced in the decay of a τ lepton are not included in the definition of the fiducial region. Nonfiducial events, i.e., events selected at the reconstructed level that do not satisfy the fiducial requirements, are included as background processes in the simultaneous fit.

Inclusive cross section measurements for the EW $W^{\pm}W^{\pm}$, EW+QCD $W^{\pm}W^{\pm}$, EW WZ, QCD WZ, and EW+QCD WZ processes, and the theoretical predictions are summarized in Table 5. To perform absolute and normalized differential production cross section measurements, signal templates from different bins of differential-basis observable values predicted by the event generator are built. Each signal template is considered as a separate process in the simultaneous binned maximum-likelihood fit. In the normalized cross section measurements, the individual cross sections in every fiducial region and the total production cross section are simultaneously evaluated, reducing the systematic uncertainties. The signal extraction at reconstruction level and the unfolding into the generator level bins are performed in a single step in the simultaneous fit. The bin migration effects due to the detector resolution

Table 3

List and description of all the input variables used in the BDT analysis for the WZ SR.

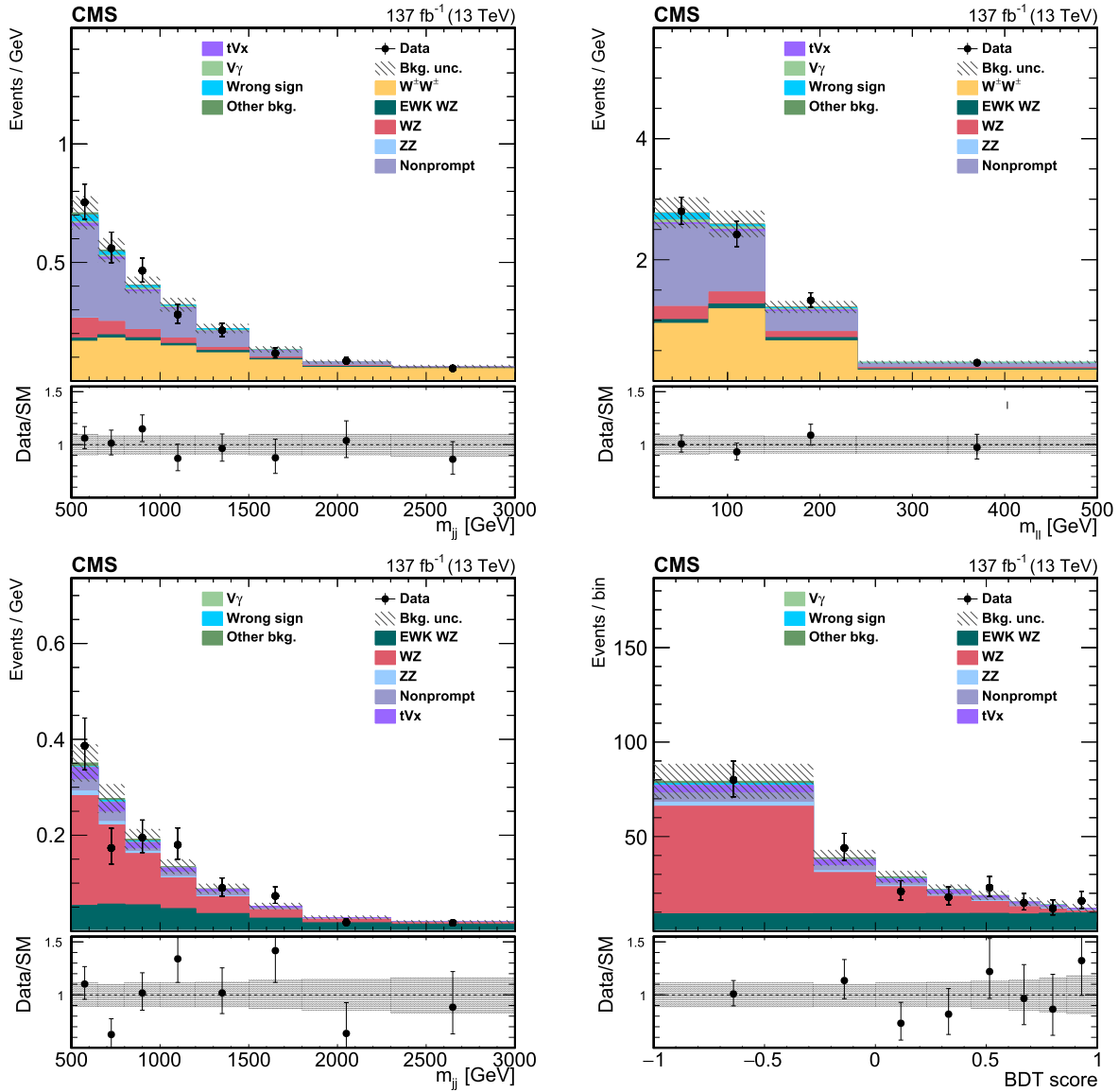| Variable	Definition
m_{jj}	Mass of the leading and trailing jets system
$|\Delta \eta_{jj}|$	Absolute difference in rapidity of the leading and trailing jets
$\Delta \phi_{jj}$	Absolute difference in azimuthal angles of the leading and trailing jets
p_T^{j1}	p_T of the leading jet
p_T^{j2}	p_T of the trailing jet
η^{j1}	Pseudorapidity of the leading jet
$|\eta^W - \eta^Z|$	Absolute difference between the rapidities of the Z boson and the charged lepton from the decay of the W boson
$z_{\ell_i}^* (i = 1 - 3)$	Zeppenfeld variable of the three selected leptons
$z_{3\ell}^*$	Zeppenfeld variable of the vector sum of the three leptons
$\Delta R_{j1,Z}$	ΔR between the leading jet and the Z boson
$|\vec{p}_T^{\,tot}| / \sum_i p_T^i$	Transverse component of the vector sum of the bosons and tagging jets momenta, normalized to their scalar p_T sum

Fig. 3. Distributions of m_{jj} (upper left) and $m_{\ell\ell}$ (upper right) in the $W^\pm W^\pm$ SR, and the distributions of m_{jj} (lower left) and BDT score (lower right) in the WZ SR. The predicted yields are shown with their best fit normalizations from the simultaneous fit. Vertical bars on data points represent the statistical uncertainty in the data. The contribution of the QCD $W^\pm W^\pm$ process is included together with the EW $W^\pm W^\pm$ process. The histograms for tVx backgrounds include the contributions from $t\bar{t}V$ and tZq processes. The histograms for other backgrounds include the contributions from double parton scattering and VVV processes. The histograms for wrong-sign background include the contributions from oppositely charged dilepton final states from $t\bar{t}$, tW, W^+W^-, and Drell–Yan processes. The overflow is included in the last bin. The bottom panel in each figure shows the ratio of the number of events observed in data to that of the total SM prediction. The gray bands represent the uncertainties in the predicted yields.

Table 4

Expected yields from SM processes and observed data events in $W^{\pm}W^{\pm}$ and WZ SRs. The combination of the statistical and systematic uncertainties is shown. The expected yields are shown with their best fit normalizations from the simultaneous fit to the Asimov data set and to the data. The signal yields do not include the QCD and EW NLO corrections.

Process	$W^{\pm}W^{\pm}$ SR		WZ SR	
	Asimov data set	Data	Asimov data set	Data
EW $W^{\pm}W^{\pm}$	209 ± 26	210 ± 26	–	–
QCD $W^{\pm}W^{\pm}$	13.8 ± 1.6	13.7 ± 2.2	–	–
Interference $W^{\pm}W^{\pm}$	8.4 ± 2.3	8.7 ± 2.3	–	–
EW WZ	14.1 ± 4.0	17.8 ± 3.9	54 ± 15	69 ± 15
QCD WZ	43 ± 6.7	42.7 ± 7.4	118 ± 17	117 ± 17
Interference WZ	0.3 ± 0.1	0.3 ± 0.2	2.2 ± 0.9	2.7 ± 1.0
ZZ	0.7 ± 0.2	0.7 ± 0.2	6.1 ± 1.7	6.0 ± 1.8
Nonprompt	211 ± 43	193 ± 40	14.6 ± 7.4	14.4 ± 6.7
tVx	7.8 ± 1.9	7.4 ± 2.2	15.1 ± 2.7	14.3 ± 2.8
$W\gamma$	9.0 ± 1.8	9.1 ± 2.9	1.1 ± 0.3	1.1 ± 0.4
Wrong-sign	13.5 ± 6.5	13.9 ± 6.5	1.6 ± 0.5	1.7 ± 0.7
Other background	5.0 ± 1.3	5.2 ± 2.1	3.3 ± 0.6	3.3 ± 0.7
Total SM	535 ± 52	522 ± 49	216 ± 21	229 ± 23
Data		524		229

Table 5

The measured inclusive cross sections for the EW $W^{\pm}W^{\pm}$, EW+QCD $W^{\pm}W^{\pm}$, EW WZ, EW+QCD WZ, and QCD WZ processes and the theoretical predictions with MadGraph5_amc@nlo at LO. The EW processes include the corresponding interference contributions. The theoretical uncertainties include statistical, PDF, and scale uncertainties. Predictions with applying the $O(\alpha_S\alpha^6)$ and $O(\alpha^7)$ corrections to the MadGraph5_amc@nlo LO cross sections, as described in the text, are also shown. The predictions of the QCD $W^{\pm}W^{\pm}$ and WZ processes do not include additional corrections. All reported values are in fb.

Process	$\sigma \mathcal{B}$ (fb)	Theoretical prediction without NLO corrections (fb)	Theoretical prediction with NLO corrections (fb)
EW $W^{\pm}W^{\pm}$	3.98 ± 0.45 $0.37\,(\text{stat}) \pm 0.25\,(\text{syst})$	3.93 ± 0.57	3.31 ± 0.47
EW+QCD $W^{\pm}W^{\pm}$	4.42 ± 0.47 $0.39\,(\text{stat}) \pm 0.25\,(\text{syst})$	4.34 ± 0.69	3.72 ± 0.59
EW WZ	1.81 ± 0.41 $0.39\,(\text{stat}) \pm 0.14\,(\text{syst})$	1.41 ± 0.21	1.24 ± 0.18
EW+QCD WZ	4.97 ± 0.46 $0.40\,(\text{stat}) \pm 0.23\,(\text{syst})$	4.54 ± 0.90	4.36 ± 0.88
QCD WZ	3.15 ± 0.49 $0.45\,(\text{stat}) \pm 0.18\,(\text{syst})$	3.12 ± 0.70	3.12 ± 0.70

are negligible. The measurement is compared with the MadGraph5_amc@nlo predictions at LO. The MadGraph5_amc@nlo predictions including the $O(\alpha_S\alpha^6)$ and $O(\alpha^7)$ corrections in the EW $W^{\pm}W^{\pm}$ and WZ processes are also included in Table 5. The measured absolute and normalized $W^{\pm}W^{\pm}$ differential cross sections in bins of m_{jj}, $m_{\ell\ell}$, and leading lepton p_T (p_T^{max}) are shown in Fig. 4. The absolute cross sections are shown in fb per GeV, while the normalized cross sections are shown in units of 1/bin. The p_T^{max} differential cross section measurements are performed by replacing the $m_{\ell\ell}$ variable by the p_T^{max} variable in the $W^{\pm}W^{\pm}$ SR in the simultaneous fit. The measured absolute and normalized WZ differential cross sections in bins of m_{jj} are shown in Fig. 5. The m_{jj} differential cross section measurements are estimated by replacing the BDT variable by the m_{jj} variable with 8 bins ([500, 650, 800, 1000, 1200, 1500, 1800, 2300, ∞] GeV) in the WZ SR in the simultaneous fit. The measured cross section values agree with the theoretical predictions within the uncertainties.

8.2. Limits on anomalous quartic gauge couplings

The events in the $W^{\pm}W^{\pm}$ and WZ SRs are used to constrain aQGCs in the effective field theory (EFT) framework [77]. Nine independent charge-conjugate and parity conserving dimension-8 effective operators are considered [14]. The S0 and S1 operators

are constructed from the covariant derivative of the Higgs doublet. The T0, T1, and T2 operators are constructed from the $SU_L(2)$ gauge fields. The mixed operators M0, M1, M6, and M7 involve the $SU_L(2)$ gauge fields and the Higgs doublet.

A nonzero aQGC enhances the production cross section at large masses of the $W^{\pm}W^{\pm}$ and WZ systems with respect to the SM prediction. The diboson transverse mass, defined as

$$m_T(VV) = \sqrt{\left(\sum_i E_i\right)^2 - \left(\sum_i p_{z,i}\right)^2}, \qquad (2)$$

where E_i and $p_{z,i}$ are the energies and longitudinal components of the momenta of the leptons and neutrinos from the decay of the gauge bosons in the event, is used in the fit for both $W^{\pm}W^{\pm}$ and WZ processes. The four-momentum of the neutrino system is defined using the $\vec{p}_T^{\,miss}$, assuming that the values of the longitudinal component of the momentum and the invariant mass are zero.

A two-dimensional distribution is used in the fit for the $W^{\pm}W^{\pm}$ process with 5 bins in $m_T(WW)$ ([0, 350, 650, 850, 1050, ∞] GeV) and 4 bins in m_{jj} ([500, 800, 1200, 1800, ∞] GeV). The SM WZ contribution is considered to be background. Similarly, a two-dimensional distribution is used in the fit for the WZ process with 5 bins in $m_T(WZ)$ ([0, 400, 750, 1050, 1350, ∞] GeV) and 2 bins in m_{jj} ([500, 1200, ∞] GeV). The m_{jj} distribution is used for the nonprompt lepton, tZq, and ZZ CRs in both fits with 4 bins ([500, 800,
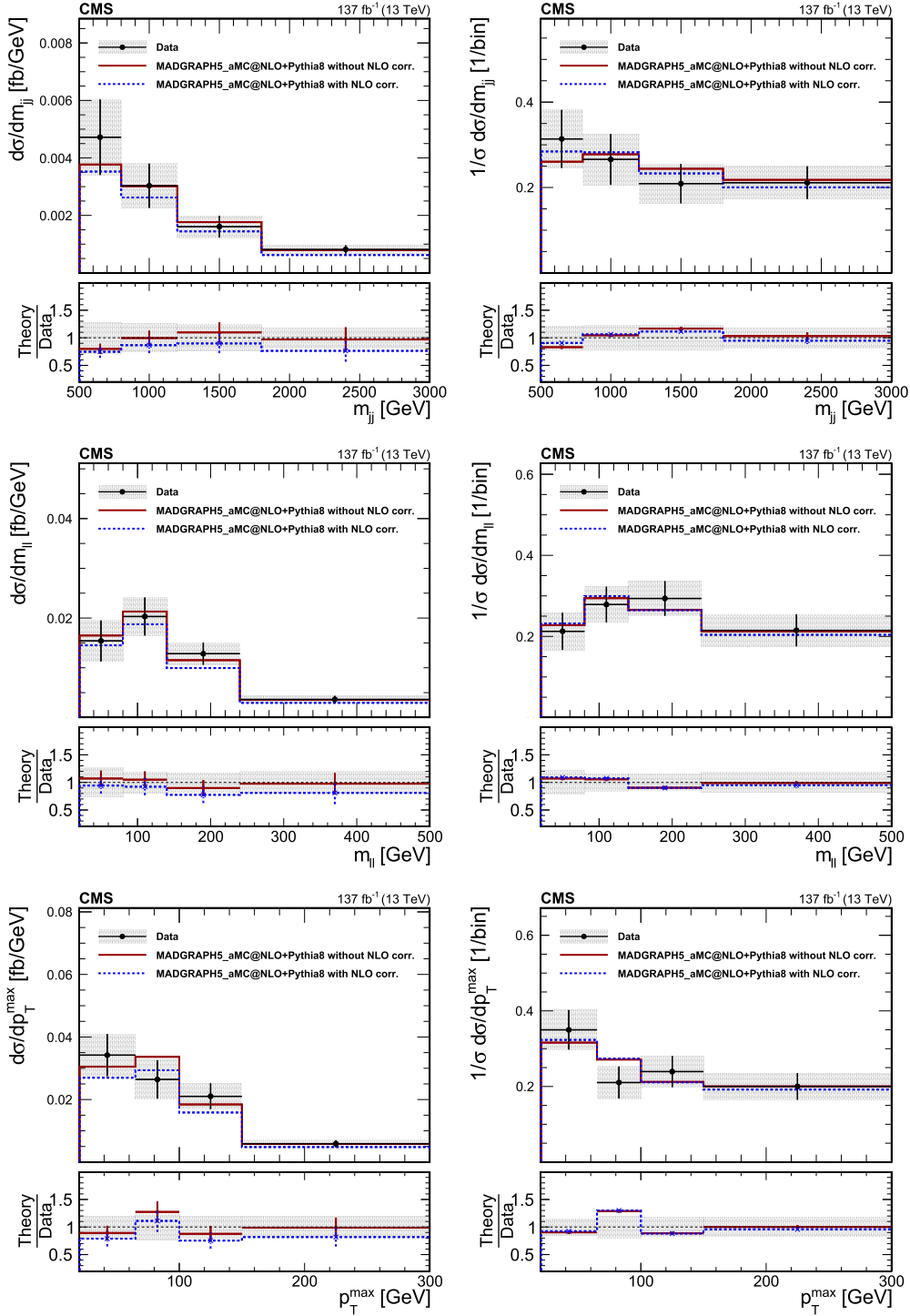
Fig. 4. The measured absolute (left) and normalized (right) $W^{\pm}W^{\pm}$ cross section measurements in bins of m_{jj} (upper), $m_{\ell\ell}$ (middle), and p_T^{max} (lower). The ratios of the predictions to the data are also shown. The measurements are compared with the predictions from MADGRAPH5_AMC@NLO at LO. The shaded bands around the data points correspond to the measurement uncertainty. The error bars around the predictions correspond to the combined statistical, PDF, and scale uncertainties. Predictions with applying the $O(\alpha_S\alpha^6)$ and $O(\alpha^7)$ corrections to the MADGRAPH5_AMC@NLO LO cross sections, as described in the text, are also shown (dashed blue).

1200, 1800, ∞] GeV). The distributions of $m_T(VV)$ in the $W^{\pm}W^{\pm}$ and WZ SRs are shown in Fig. 6.

No excess of events with respect to the SM background predictions is observed. The observed and expected 95% confidence level (CL) lower and upper limits on the aQGC parameters f/Λ^4, where f is the dimensionless coefficient of the given operator and Λ is the energy scale of new physics, are derived from a modified frequentist approach with the CL$_s$ criterion [73,74] and asymptotic re-

sults for the test statistic [76]. The expected cross section depends quadratically on aQGC, therefore the expected yields are calculated from a parabolic interpolation from the discrete coupling parameters of the simulated signals. Table 6 shows the individual lower and upper limits for the coefficients of the T0, T1, T2, M0, M1, M6, M7, S0, and S1 operators obtained by setting all other aQGCs parameters to zero for the $W^{\pm}W^{\pm}$ and WZ channels, and their combination. The results are sensitive to the number of data events
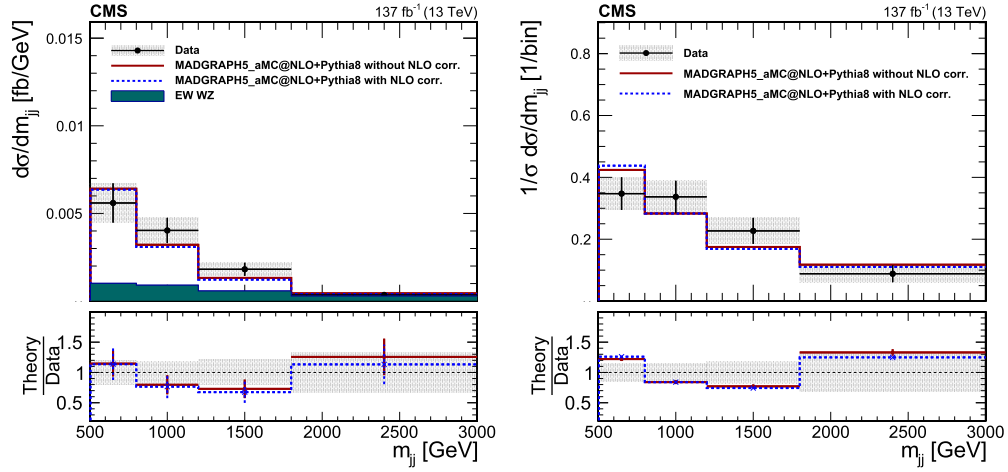
Fig. 5. The measured absolute (left) and normalized (right) WZ cross section measurements in bins of m_{jj}. The ratios of the predictions to the data are also shown. The measurements are compared with the predictions from MADGRAPH5_AMC@NLO at LO. The shaded bands around the data points correspond to the measurement uncertainty. The error bars around the predictions correspond to the combined statistical, PDF, and scale uncertainties. Predictions with applying the $O(\alpha_S\alpha^6)$ and $O(\alpha^7)$ corrections to the MADGRAPH5_AMC@NLO LO cross sections, as described in the text, are shown (dashed blue). The MADGRAPH5_AMC@NLO predictions in the EW total cross sections are also shown (dark cyan).

Table 6
Observed and expected lower and upper 95% CL limits on the parameters of the quartic operators T0, T1, T2, M0, M1, M6, M7, S0, and S1 in $W^{\pm}W^{\pm}$ and WZ channels, obtained without using any unitarization procedure. The last two columns show the observed and expected limits for the combination of the $W^{\pm}W^{\pm}$ and WZ channels. Results are obtained by setting all other aQGCs parameters to zero.

	Observed ($W^{\pm}W^{\pm}$) (TeV^{-4})	Expected ($W^{\pm}W^{\pm}$) (TeV^{-4})	Observed (WZ) (TeV^{-4})	Expected (WZ) (TeV^{-4})	Observed (TeV^{-4})	Expected (TeV^{-4})
f_{T0}/Λ^4	[-0.28, 0.31]	[-0.36, 0.39]	[-0.62, 0.65]	[-0.82, 0.85]	[-0.25, 0.28]	[-0.35, 0.37]
f_{T1}/Λ^4	[-0.12, 0.15]	[-0.16, 0.19]	[-0.37, 0.41]	[-0.49, 0.55]	[-0.12, 0.14]	[-0.16, 0.19]
f_{T2}/Λ^4	[-0.38, 0.50]	[-0.50, 0.63]	[-1.0 , 1.3]	[-1.4, 1.7]	[-0.35, 0.48]	[-0.49, 0.63]
f_{M0}/Λ^4	[-3.0, 3.2]	[-3.7, 3.8]	[-5.8, 5.8]	[-7.6, 7.6]	[-2.7, 2.9]	[-3.6, 3.7]
f_{M1}/Λ^4	[-4.7, 4.7]	[-5.4, 5.8]	[-8.2, 8.3]	[-11, 11]	[-4.1, 4.2]	[-5.2, 5.5]
f_{M6}/Λ^4	[-6.0, 6.5]	[-7.5, 7.6]	[-12, 12]	[-15, 15]	[-5.4, 5.8]	[-7.2, 7.3]
f_{M7}/Λ^4	[-6.7, 7.0]	[-8.3, 8.1]	[-10, 10]	[-14, 14]	[-5.7, 6.0]	[-7.8, 7.6]
f_{S0}/Λ^4	[-6.0, 6.4]	[-6.0, 6.2]	[-19, 19]	[-24, 24]	[-5.7, 6.1]	[-5.9, 6.2]
f_{S1}/Λ^4	[-18, 19]	[-18, 19]	[-30, 30]	[-38, 39]	[-16, 17]	[-18, 18]

Table 7
Observed and expected lower and upper 95% CL limits on the parameters of the quartic operators T0, T1, T2, M0, M1, M6, M7, S0, and S1 in $W^{\pm}W^{\pm}$ and WZ channels by cutting the EFT expansion at the unitarity limit. The last two columns show the observed and expected limits for the combination of the $W^{\pm}W^{\pm}$ and WZ channels. Results are obtained by setting all other aQGCs parameters to zero.

	Observed ($W^{\pm}W^{\pm}$) (TeV^{-4})	Expected ($W^{\pm}W^{\pm}$) (TeV^{-4})	Observed (WZ) (TeV^{-4})	Expected (WZ) (TeV^{-4})	Observed (TeV^{-4})	Expected (TeV^{-4})
f_{T0}/Λ^4	[-1.5, 2.3]	[-2.1, 2.7]	[-1.6, 1.9]	[-2.0, 2.2]	[-1.1, 1.6]	[-1.6, 2.0]
f_{T1}/Λ^4	[-0.81, 1.2]	[-0.98, 1.4]	[-1.3, 1.5]	[-1.6, 1.8]	[-0.69, 0.97]	[-0.94, 1.3]
f_{T2}/Λ^4	[-2.1, 4.4]	[-2.7, 5.3]	[-2.7, 3.4]	[-4.4, 5.5]	[-1.6, 3.1]	[-2.3, 3.8]
f_{M0}/Λ^4	[-13, 16]	[-19, 18]	[-16, 16]	[-19, 19]	[-11, 12]	[-15, 15]
f_{M1}/Λ^4	[-20, 19]	[-22, 25]	[-19, 20]	[-23, 24]	[-15, 14]	[-18, 20]
f_{M6}/Λ^4	[-27, 32]	[-37, 37]	[-34, 33]	[-39, 39]	[-22, 25]	[-31, 30]
f_{M7}/Λ^4	[-22, 24]	[-27, 25]	[-22, 22]	[-28, 28]	[-16, 18]	[-22, 21]
f_{S0}/Λ^4	[-35, 36]	[-31, 31]	[-83, 85]	[-88, 91]	[-34, 35]	[-31, 31]
f_{S1}/Λ^4	[-100, 120]	[-100, 110]	[-110, 110]	[-120, 130]	[-86, 99]	[-91, 97]

with large $m_T(VV)$ values. These results are about a factor of two more restrictive than the previous analyses of the leptonic decay modes of the $W^{\pm}W^{\pm}$ and WZ processes [21,24]. However, the results are less restrictive than the analysis using the semileptonic final states [28]. No unitarization procedure is applied to obtain these results.

The EFT is not a complete model and the presence of nonzero aQGCs will violate tree-level unitarity at sufficiently high energy. More physical limits can be obtained by cutting the EFT integration at the unitarity limit and adding the expected SM contribution for generated events with VV invariant masses above the unitarity limit [78]. The unitarity limits for each aQGC parameter, typically about 1.5 TeV, are calculated using VBFNLO 1.4.0 [79–81] after applying the appropriate Wilson coefficient conversion factors. Table 7 shows the individual lower and upper limits for the coefficients of the T0, T1, T2, M0, M1, M6, M7, S0, and S1 operators by cutting off the EFT expansion at the unitarity limit. These limits are significantly less stringent compared with the limits in Table 6, where the unitarity violation is not considered.
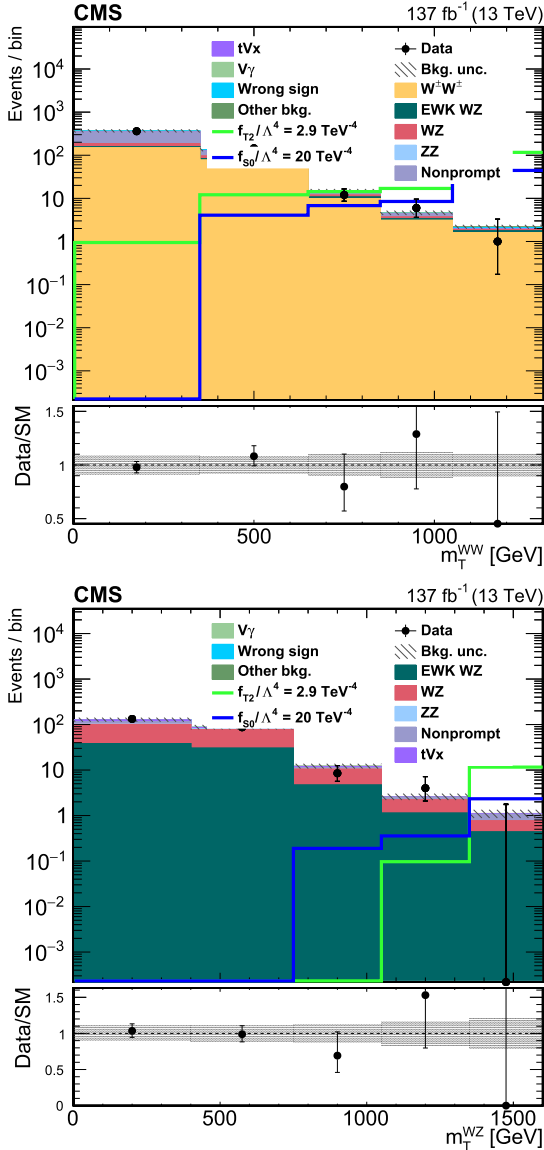
Fig. 6. Distributions of $m_T(WW)$ (upper) in the $W^\pm W^\pm$ SR and $m_T(WZ)$ (lower) in the WZ SR. The gray bands include uncertainties from the predicted yields. The SM predicted yields are shown with their best fit normalizations from the corresponding fits. The contribution of the QCD $W^\pm W^\pm$ process is included together with the EW $W^\pm W^\pm$ process. The overflow is included in the last bin. The bottom panel in each figure shows the ratio of the number of events observed in data to the total SM prediction. The solid lines show the signal predictions for two illustrative aQGC parameters.

9. Summary

The production cross sections of WZ and same-sign WW boson pairs in association with two jets are measured in proton-proton collisions at a center-of-mass energy of 13 TeV. The data sample corresponds to an integrated luminosity of $137\,\mathrm{fb}^{-1}$, collected with the CMS detector during 2016–18. The measurements are performed in the leptonic decay modes $W^\pm Z \to \ell^\pm \nu \ell'^\pm \ell'^\mp$ and $W^\pm W^\pm \to \ell^\pm \nu \ell'^\pm \nu$, where $\ell, \ell' = e$, μ. An observation of electroweak production of WZ boson pairs is reported with an observed (expected) significance of 6.8 (5.3) standard deviations. Differential cross sections as functions of the invariant masses of the jet and charged lepton pairs, as well as the leading-lepton transverse momentum, are measured for $W^\pm W^\pm$ production and are compared to the standard model predictions. Differential cross

sections as a function of the invariant mass of the jet pair are also measured for WZ production. Stringent limits are set in the framework of effective field theory, with and without consideration of tree-level unitarity violation, on the dimension-8 operators T0, T1, T2, M0, M1, M6, M7, S0, and S1.

Declaration of competing interest

The authors declare that they have no known competing financial interests or personal relationships that could have appeared to influence the work reported in this paper.

References

[1] ATLAS Collaboration, Observation of a new particle in the search for the standard model Higgs boson with the ATLAS detector at the LHC, Phys. Lett. B 716 (2012) 1, https://doi.org/10.1016/j.physletb.2012.08.020, arXiv:1207.7214.

[2] CMS Collaboration, Observation of a new boson at a mass of 125 GeV with the CMS experiment at the LHC, Phys. Lett. B 716 (2012) 30, https://doi.org/10.1016/j.physletb.2012.08.021, arXiv:1207.7235.

[3] CMS Collaboration, Observation of a new boson with mass near 125 GeV in pp collisions at $\sqrt{s}$ = 7 and 8 TeV, J. High Energy Phys. 06 (2013) 081, https://doi.org/10.1007/JHEP06(2013)081, arXiv:1303.4571.

[4] F. Englert, R. Brout, Broken symmetry and the mass of gauge vector mesons, Phys. Rev. Lett. 13 (1964) 321, https://doi.org/10.1103/PhysRevLett.13.321.

[5] P.W. Higgs, Broken symmetries, massless particles and gauge fields, Phys. Lett. 12 (1964) 132, https://doi.org/10.1016/0031-9163(64)91136-9.

[6] P.W. Higgs, Broken symmetries and the masses of gauge bosons, Phys. Rev. Lett. 13 (1964) 508, https://doi.org/10.1103/PhysRevLett.13.508.

[7] G.S. Guralnik, C.R. Hagen, T.W.B. Kibble, Global conservation laws and massless particles, Phys. Rev. Lett. 13 (1964) 585, https://doi.org/10.1103/PhysRevLett.13.585.

[8] P.W. Higgs, Spontaneous symmetry breakdown without massless bosons, Phys. Rev. 145 (1966) 1156, https://doi.org/10.1103/PhysRev.145.1156.

[9] T.W.B. Kibble, Symmetry breaking in non-Abelian gauge theories, Phys. Rev. 155 (1967) 1554, https://doi.org/10.1103/PhysRev.155.1554.

[10] D. Espriu, B. Yencho, Longitudinal WW scattering in light of the Higgs boson discovery, Phys. Rev. D 87 (2013) 055017, https://doi.org/10.1103/PhysRevD.87.055017, arXiv:1212.4158.

[11] J. Chang, K. Cheung, C.-T. Lu, T.-C. Yuan, WW scattering in the era of post-Higgs-boson discovery, Phys. Rev. D 87 (2013) 093005, https://doi.org/10.1103/PhysRevD.87.093005, arXiv:1303.6335.

[12] B.W. Lee, C. Quigg, H.B. Thacker, The strength of weak interactions at very high-energies and the Higgs boson mass, Phys. Rev. Lett. 38 (1977) 883, https://doi.org/10.1103/PhysRevLett.38.883.

[13] B.W. Lee, C. Quigg, H.B. Thacker, Weak interactions at very high-energies: the role of the Higgs boson mass, Phys. Rev. D 16 (1977) 1519, https://doi.org/10.1103/PhysRevD.16.1519.

[14] O.J.P. Éboli, M.C. Gonzalez-Garcia, J.K. Mizukoshi, pp $\rightarrow$ jj$e^{\pm}\mu^{\pm}\nu\nu$ and jj$e^{\pm}\mu^{\mp}\nu\nu$ at $O(\alpha_{em}^6)$ and $O(\alpha_{em}^4\alpha_s^2)$ for the study of the quartic electroweak gauge boson vertex at CERN LHC, Phys. Rev. D 74 (2006) 073005, https://doi.org/10.1103/PhysRevD.74.073005, arXiv:hep-ph/0606118.

[15] CMS Collaboration, CMS luminosity measurement for the 2016 data-taking period, CMS Physics Analysis Summary CMS-PAS-LUM-17-001, https://cds.cern.ch/record/2138682, 2017.

[16] CMS Collaboration, CMS luminosity measurement for the 2017 data-taking period at $\sqrt{s}$ = 13 TeV, CMS Physics Analysis Summary CMS-PAS-LUM-17-004, https://cds.cern.ch/record/2621960, 2017.

[17] CMS Collaboration, CMS luminosity measurement for the 2018 data-taking period at $\sqrt{s}$ = 13 TeV, CMS Physics Analysis Summary CMS-PAS-LUM-18-002, https://cds.cern.ch/record/2676164, 2018.

[18] CMS Collaboration, The CMS experiment at the CERN LHC, J. Instrum. 3 (2008) S08004, https://doi.org/10.1088/1748-0221/3/08/S08004.

[19] CMS Collaboration, Study of vector boson scattering and search for new physics in events with two same-sign leptons and two jets, Phys. Rev. Lett. 114 (2015) 051801, https://doi.org/10.1103/PhysRevLett.114.051801, arXiv:1410.6315.

[20] ATLAS Collaboration, Evidence for electroweak production of $W^{\pm}W^{\pm}$jj in pp collisions at $\sqrt{s}$ = 8 TeV with the ATLAS detector, Phys. Rev. Lett. 113 (2014) 141803, https://doi.org/10.1103/PhysRevLett.113.141803, arXiv:1405.6241.

[21] CMS Collaboration, Observation of electroweak production of same-sign W boson pairs in the two jet and two same-sign lepton final state in proton-proton collisions at $\sqrt{s}$ = 13 TeV, Phys. Rev. Lett. 120 (2018) 081801, https://doi.org/10.1103/PhysRevLett.120.081801, arXiv:1709.05822.

[22] ATLAS Collaboration, Observation of electroweak production of a same-sign W boson pair in association with two jets in pp collisions at $\sqrt{s}$ = 13 TeV with the ATLAS detector, Phys. Rev. Lett. 123 (2019) 161801, https://doi.org/10.1103/PhysRevLett.123.161801, arXiv:1906.03203.

[23] ATLAS Collaboration, Measurements of $W^{\pm}Z$ production cross sections in pp collisions at $\sqrt{s}$ = 8 TeV with the ATLAS detector and limits on anomalous gauge boson self-couplings, Phys. Rev. D 93 (2016) 092004, https://doi.org/10.1103/PhysRevD.93.092004, arXiv:1603.02151.

[24] CMS Collaboration, Measurement of electroweak WZ boson production and search for new physics in WZ + two jets events in pp collisions at $\sqrt{s}$ = 13 TeV, Phys. Lett. B 795 (2019) 281, https://doi.org/10.1016/j.physletb.2019.05.042, arXiv:1901.04060.

[25] ATLAS Collaboration, Observation of electroweak $W^{\pm}Z$ boson pair production in association with two jets in pp collisions at $\sqrt{s}$ = 13 TeV with the ATLAS detector, Phys. Lett. B 793 (2019) 469, https://doi.org/10.1016/j.physletb.2019.05.012, arXiv:1812.09740.

[26] ATLAS Collaboration, Search for the electroweak diboson production in association with a high-mass dijet system in semileptonic final states in pp collisions at $\sqrt{s}$ = 13 TeV with the ATLAS detector, Phys. Rev. D 100 (2019) 032007, https://doi.org/10.1103/PhysRevD.100.032007, arXiv:1905.07714.

[27] ATLAS Collaboration, Search for anomalous electroweak production of WW/WZ in association with a high-mass dijet system in pp collisions at $\sqrt{s}$ = 8 TeV with the ATLAS detector, Phys. Rev. D 95 (2017) 032001, https://doi.org/10.1103/PhysRevD.95.032001, arXiv:1609.05122.

[28] CMS Collaboration, Search for anomalous electroweak production of vector boson pairs in association with two jets in proton-proton collisions at 13 TeV, Phys. Lett. B 798 (2019) 134985, https://doi.org/10.1016/j.physletb.2019.134985, arXiv:1905.07445.

[29] CMS Collaboration, The CMS trigger system, J. Instrum. 12 (2017) P01020, https://doi.org/10.1088/1748-0221/12/01/P01020, arXiv:1609.02366.

[30] J. Alwall, R. Frederix, S. Frixione, V. Hirschi, F. Maltoni, O. Mattelaer, H.S. Shao, T. Stelzer, P. Torrielli, M. Zaro, The automated computation of tree-level and next-to-leading order differential cross sections, and their matching to parton shower simulations, J. High Energy Phys. 07 (2014) 079, https://doi.org/10.1007/JHEP07(2014)079, arXiv:1405.0301.

[31] J. Alwall, M. Herquet, F. Maltoni, O. Mattelaer, T. Stelzer, MadGraph 5: going beyond, J. High Energy Phys. 06 (2011) 128, https://doi.org/10.1007/JHEP06(2011)128, arXiv:1106.0522.

[32] R. Frederix, S. Frixione, Merging meets matching in MC@NLO, J. High Energy Phys. 12 (2012) 061, https://doi.org/10.1007/JHEP12(2012)061, arXiv:1209.6215.

[33] P. Artoisenet, V. Lemaitre, F. Maltoni, O. Mattelaer, Automation of the matrix element reweighting method, J. High Energy Phys. 12 (2010) 068, https://doi.org/10.1007/JHEP12(2010)068, arXiv:1007.3300.

[34] J. Alwall, S. Höche, F. Krauss, N. Lavesson, L. Lönnblad, F. Maltoni, M.L. Mangano, M. Moretti, C.G. Papadopoulos, F. Piccinini, S. Schumann, M. Treccani, J. Winter, M. Worek, Comparative study of various algorithms for the merging of parton showers and matrix elements in hadronic collisions, Eur. Phys. J. C 53 (2008) 473, https://doi.org/10.1140/epjc/s10052-007-0490-5, arXiv:0706.2569.

[35] M. Grazzini, S. Kallweit, D. Rathlev, M. Wiesemann, $W^{\pm}Z$ production at hadron colliders in NNLO QCD, Phys. Lett. B 761 (2016) 179, https://doi.org/10.1016/j.physletb.2016.08.017, arXiv:1604.08576.

[36] B. Biedermann, A. Denner, M. Pellen, Large electroweak corrections to vector boson scattering at the large hadron collider, Phys. Rev. Lett. 118 (2017) 261801, https://doi.org/10.1103/PhysRevLett.118.261801, arXiv:1611.02951.

[37] B. Biedermann, A. Denner, M. Pellen, Complete NLO corrections to W^+W^+ scattering and its irreducible background at the LHC, J. High Energy Phys. 10 (2017) 124, https://doi.org/10.1007/JHEP10(2017)124, arXiv:1708.00268.

[38] A. Denner, S. Dittmaier, P. Maierhöfer, M. Pellen, C. Schwan, QCD and electroweak corrections to WZ scattering at the LHC, J. High Energy Phys. 06 (2019) 067, https://doi.org/10.1007/JHEP06(2019)067, arXiv:1904.00882.

[39] A. Ballestrero, et al., Precise predictions for same-sign W-boson scattering at the LHC, Eur. Phys. J. C 78 (2018) 671, https://doi.org/10.1140/epjc/s10052-018-6136-y, arXiv:1803.07943.

[40] S. Frixione, B.R. Webber, Matching NLO QCD computations and parton shower simulations, J. High Energy Phys. 06 (2002) 029, https://doi.org/10.1088/1126-6708/2002/06/029, arXiv:hep-ph/0204244.

[41] P. Nason, A new method for combining NLO QCD with shower Monte Carlo algorithms, J. High Energy Phys. 11 (2004) 040, https://doi.org/10.1088/1126-6708/2004/11/040, arXiv:hep-ph/0409146.

[42] S. Frixione, P. Nason, C. Oleari, Matching NLO QCD computations with parton shower simulations: the POWHEG method, J. High Energy Phys. 11 (2007) 070, https://doi.org/10.1088/1126-6708/2007/11/070, arXiv:0709.2092.

[43] S. Alioli, P. Nason, C. Oleari, E. Re, NLO vector-boson production matched with shower in POWHEG, J. High Energy Phys. 07 (2008) 060, https://doi.org/10.1088/1126-6708/2008/07/060, arXiv:0805.4802.

[44] S. Alioli, P. Nason, C. Oleari, E. Re, A general framework for implementing NLO calculations in shower Monte Carlo programs: the POWHEG BOX, J. High Energy Phys. 06 (2010) 043, https://doi.org/10.1007/JHEP06(2010)043, arXiv:1002.2581.

[45] CMS Collaboration, Measurement of the associated production of a single top quark and a Z boson in pp collisions at $\sqrt{s} = 13$ TeV, Phys. Lett. B 779 (2018) 358, https://doi.org/10.1016/j.physletb.2018.02.025, arXiv:1712.02825.

[46] T. Sjöstrand, S. Ask, J.R. Christiansen, R. Corke, N. Desai, P. Ilten, S. Mrenna, S. Prestel, C.O. Rasmussen, P.Z. Skands, An introduction to PYTHIA 8.2, Comput. Phys. Commun. 191 (2015) 159, https://doi.org/10.1016/j.cpc.2015.01.024, arXiv:1410.3012.

[47] R.D. Ball, et al., NNPDF, Parton distributions for the LHC Run II, J. High Energy Phys. 04 (2015) 040, https://doi.org/10.1007/JHEP04(2015)040, arXiv: 1410.8849.

[48] R.D. Ball, et al., NNPDF, Parton distributions from high-precision collider data, Eur. Phys. J. C 77 (2017) 663, https://doi.org/10.1140/epjc/s10052-017-5199-5, arXiv:1706.00428.

[49] P. Skands, S. Carrazza, J. Rojo, Tuning PYTHIA 8.1: the Monash 2013 tune, Eur. Phys. J. C 74 (2014) 3024, https://doi.org/10.1140/epjc/s10052-014-3024-y, arXiv:1404.5630.

[50] CMS Collaboration, Event generator tunes obtained from underlying event and multiparton scattering measurements, Eur. Phys. J. C 76 (2016) 155, https://doi.org/10.1140/epjc/s10052-016-3988-x, arXiv:1512.00815.

[51] CMS Collaboration, Extraction and validation of a new set of CMS PYTHIA8 tunes from underlying-event measurements, Eur. Phys. J. C 80 (2020) 4, https://doi.org/10.1140/epjc/s10052-019-7499-4, arXiv:1903.12179.

[52] S. Agostinelli, et al., Geant4, GEANT4 — a simulation toolkit, Nucl. Instrum. Methods Phys. Res., Sect. A, Accel. Spectrom. Detect. Assoc. Equip. 506 (2003) 250, https://doi.org/10.1016/S0168-9002(03)01368-8.

[53] CMS Collaboration, Particle-flow reconstruction and global event description with the CMS detector, J. Instrum. 12 (2017) P10003, https://doi.org/10.1088/1748-0221/12/10/P10003, arXiv:1706.04965.

[54] M. Cacciari, G.P. Salam, G. Soyez, The anti-k_T jet clustering algorithm, J. High Energy Phys. 04 (2008) 063, https://doi.org/10.1088/1126-6708/2008/04/063, arXiv:0802.1189.

[55] CMS Collaboration, Jet energy scale and resolution in the CMS experiment in pp collisions at 8 TeV, J. Instrum. 12 (2017) P02014, https://doi.org/10.1088/1748-0221/12/02/P02014, arXiv:1607.03663.

[56] CMS Collaboration, Jet energy scale and resolution performance with 13 TeV data collected by CMS in 2016-2018, CMS Detector Performance Summary CMS-DP-2020-019, https://cds.cern.ch/record/2715872, 2020.

[57] CMS Collaboration, Pileup mitigation at CMS in 13 TeV data, 2020, accepted for publication in JINST, arXiv:2003.00503.

[58] CMS Collaboration, Performance of missing transverse momentum reconstruction in proton-proton collisions at $\sqrt{s} = 13$ TeV using the CMS detector, J. Instrum. 14 (2019) P07004, https://doi.org/10.1088/1748-0221/14/07/P07004, arXiv:1903.06078.

[59] M. Cacciari, G.P. Salam, G. Soyez, FastJet user manual, Eur. Phys. J. C 72 (2012) 1896, https://doi.org/10.1140/epjc/s10052-012-1896-2, arXiv:1111.6097.

[60] CMS Collaboration, Identification of heavy-flavour jets with the CMS detector in pp collisions at 13 TeV, J. Instrum. 13 (2018) P05011, https://doi.org/10.1088/1748-0221/13/05/P05011, arXiv:1712.07158.

[61] CMS Collaboration, Performance of electron reconstruction and selection with the CMS detector in proton-proton collisions at $\sqrt{s} = 8$ TeV, J. Instrum. 10 (2015) P06005, https://doi.org/10.1088/1748-0221/10/06/P06005, arXiv:1502.02701.

[62] CMS Collaboration, Performance of the CMS muon detector and muon reconstruction with proton-proton collisions at $\sqrt{s} = 13$ TeV, J. Instrum. 13 (2018) P06015, https://doi.org/10.1088/1748-0221/13/06/P06015, arXiv:1804.04528.

[63] CMS Collaboration, Measurements of properties of the Higgs boson decaying to a W boson pair in pp collisions at $\sqrt{s} = 13$ TeV, Phys. Lett. B 791 (2019) 96, https://doi.org/10.1016/j.physletb.2018.12.073, arXiv:1806.05246.

[64] CMS Collaboration, Performance of CMS muon reconstruction in cosmic-ray events, J. Instrum. 5 (2010) T03022, https://doi.org/10.1088/1748-0221/5/03/T03022, arXiv:0911.4994.

[65] CMS Collaboration, Performance of the reconstruction and identification of high-momentum muons in proton-proton collisions at $\sqrt{s} = 13$ TeV, J. Instrum. 15 (2020) P02027, https://doi.org/10.1088/1748-0221/15/02/P02027, arXiv:1912.03516.

[66] Particle Data Group, M. Tanabashi, et al., Review of particle physics, Phys. Rev. D 98 (2018) 030001, https://doi.org/10.1103/PhysRevD.98.030001.

[67] D.L. Rainwater, R. Szalapski, D. Zeppenfeld, Probing color singlet exchange in Z + two jet events at the CERN LHC, Phys. Rev. D 54 (1996) 6680, https://doi.org/10.1103/PhysRevD.54.6680, arXiv:hep-ph/9605444.

[68] CMS Collaboration, Electron and photon performance in CMS with the full 2017 data sample and additional 2016 highlights for the CALOR 2018 conference, CMS Detector Performance Summary CMS-DP-2018-017, https://cds.cern.ch/record/2320638, 2018.

[69] ATLAS Collaboration, Measurement of the inelastic proton-proton cross section at $\sqrt{s} = 13$ TeV with the ATLAS detector at the LHC, Phys. Rev. Lett. 117 (2016) 182002, https://doi.org/10.1103/PhysRevLett.117.182002, arXiv:1606.02625.

[70] CMS Collaboration, Measurement of the inelastic proton-proton cross section at $\sqrt{s} = 13$ TeV, J. High Energy Phys. 07 (2018) 161, https://doi.org/10.1007/JHEP07(2018)161, arXiv:1802.02613.

[71] CMS Collaboration, Measurements of differential Z boson production cross sections in proton-proton collisions at $\sqrt{s} = 13$ TeV, J. High Energy Phys. 12 (2019) 061, https://doi.org/10.1007/JHEP12(2019)061, arXiv:1909.04133.

[72] J. Butterworth, S. Carrazza, A. Cooper-Sarkar, A. De Roeck, J. Feltesse, J. Forte, Stefano Gao, S. Glazov, J. Huston, Z. Kassabov, PDF4LHC recommendations for LHC Run II, J. Phys. G 43 (2016) 023001, https://doi.org/10.1088/0954-3899/43/2/023001, arXiv:1510.03865.

[73] T. Junk, Confidence level computation for combining searches with small statistics, Nucl. Instrum. Methods Phys. Res., Sect. A, Accel. Spectrom. Detect. Assoc. Equip. 434 (1999) 435, https://doi.org/10.1016/S0168-9002(99)00498-2, arXiv:hep-ex/9902006.

[74] A.L. Read, Presentation of search results: the CL$_s$ technique, J. Phys. G 28 (2002) 2693, https://doi.org/10.1088/0954-3899/28/10/313.

[75] H. Voss, A. Höcker, J. Stelzer, F. Tegenfeldt, TMVA, the toolkit for multivariate data analysis with ROOT, in: XIth International Workshop on Advanced Computing and Analysis Techniques in Physics Research (ACAT), 2007, p. 40, arXiv:physics/0703039, PoS (ACAT) 040.

[76] G. Cowan, K. Cranmer, E. Gross, O. Vitells, Asymptotic formulae for likelihood-based tests of new physics, Eur. Phys. J. C 71 (2011) 1554, https://doi.org/10.1140/epjc/s10052-011-1554-0, arXiv:1007.1727, Erratum: https://doi.org/10.1140/epjc/s10052-013-2501-z.

[77] C. Degrande, N. Greiner, W. Kilian, O. Mattelaer, H. Mebane, T. Stelzer, S. Willenbrock, C. Zhang, Effective field theory: a modern approach to anomalous couplings, Ann. Phys. 335 (2013) 21, https://doi.org/10.1016/j.aop.2013.04.016, arXiv:1205.4231.

[78] J. Kalinowski, P. Kozow, S. Pokorski, J. Rosiek, M. Szleper, S. Tkaczyk, Same-sign WW scattering at the LHC: can we discover BSM effects before discovering new states?, Eur. Phys. J. C 78 (2018) 403, https://doi.org/10.1140/epjc/s10052-018-5885-y, arXiv:1802.02366.

[79] K. Arnold, et al., VBFNLO: a parton level Monte Carlo for processes with electroweak bosons, Comput. Phys. Commun. 180 (2009) 1661, https://doi.org/10.1016/j.cpc.2009.03.006, arXiv:0811.4559.

[80] J. Baglio, et al., VBFNLO: a parton level Monte Carlo for processes with electroweak bosons – manual for version 2.7.0, arXiv:1107.4038, 2011.

[81] J. Baglio, J. Bellm, F. Campanario, B. Feigl, J. Frank, T. Figy, M. Kerner, L.D. Ninh, S. Palmer, M. Rauch, R. Roth, F. Schissler, O. Schlimpert, D. Zeppenfeld, Release note – VBFNLO 2.7.0, arXiv:1404.3940, 2014.

The CMS Collaboration

A.M. Sirunyan [†], A. Tumasyan

Yerevan Physics Institute, Yerevan, Armenia

W. Adam, F. Ambrogi, T. Bergauer, M. Dragicevic, J. Erö, A. Escalante Del Valle, R. Frühwirth [1], M. Jeitler [1], N. Krammer, L. Lechner, D. Liko, T. Madlener, I. Mikulec, F.M. Pitters, N. Rad, J. Schieck [1], R. Schöfbeck, M. Spanring, S. Templ, W. Waltenberger, C.-E. Wulz [1], M. Zarucki

Institut für Hochenergiephysik, Wien, Austria

V. Chekhovsky, A. Litomin, V. Makarenko, J. Suarez Gonzalez

Institute for Nuclear Problems, Minsk, Belarus

M.R. Darwish[2], E.A. De Wolf, D. Di Croce, X. Janssen, T. Kello[3], A. Lelek, M. Pieters, H. Rejeb Sfar, H. Van Haevermaet, P. Van Mechelen, S. Van Putte, N. Van Remortel

Universiteit Antwerpen, Antwerpen, Belgium

F. Blekman, E.S. Bols, S.S. Chhibra, J. D'Hondt, J. De Clercq, D. Lontkovskyi, S. Lowette, I. Marchesini, S. Moortgat, A. Morton, Q. Python, S. Tavernier, W. Van Doninck, P. Van Mulders

Vrije Universiteit Brussel, Brussel, Belgium

D. Beghin, B. Bilin, B. Clerbaux, G. De Lentdecker, H. Delannoy, B. Dorney, L. Favart, A. Grebenyuk, A.K. Kalsi, I. Makarenko, L. Moureaux, L. Pétré, A. Popov, N. Postiau, E. Starling, L. Thomas, C. Vander Velde, P. Vanlaer, D. Vannerom, L. Wezenbeek

Université Libre de Bruxelles, Bruxelles, Belgium

T. Cornelis, D. Dobur, I. Khvastunov[4], M. Niedziela, C. Roskas, K. Skovpen, M. Tytgat, W. Verbeke, B. Vermassen, M. Vit

Ghent University, Ghent, Belgium

G. Bruno, F. Bury, C. Caputo, P. David, C. Delaere, M. Delcourt, I.S. Donertas, A. Giammanco, V. Lemaitre, K. Mondal, J. Prisciandaro, A. Taliercio, M. Teklishyn, P. Vischia, S. Wuyckens, J. Zobec

Université Catholique de Louvain, Louvain-la-Neuve, Belgium

G.A. Alves, G. Correia Silva, C. Hensel, A. Moraes

Centro Brasileiro de Pesquisas Fisicas, Rio de Janeiro, Brazil

W.L. Aldá Júnior, E. Belchior Batista Das Chagas, W. Carvalho, J. Chinellato[5], E. Coelho, E.M. Da Costa, G.G. Da Silveira[6], D. De Jesus Damiao, S. Fonseca De Souza, H. Malbouisson, J. Martins[7], D. Matos Figueiredo, M. Medina Jaime[8], M. Melo De Almeida, C. Mora Herrera, L. Mundim, H. Nogima, P. Rebello Teles, L.J. Sanchez Rosas, A. Santoro, S.M. Silva Do Amaral, A. Sznajder, M. Thiel, E.J. Tonelli Manganote[5], F. Torres Da Silva De Araujo, A. Vilela Pereira

Universidade do Estado do Rio de Janeiro, Rio de Janeiro, Brazil

C.A. Bernardes[a], L. Calligaris[a], T.R. Fernandez Perez Tomei[a], E.M. Gregores[b], D.S. Lemos[a], P.G. Mercadante[b], S.F. Novaes[a], Sandra S. Padula[a]

[a] *Universidade Estadual Paulista, São Paulo, Brazil*
[b] *Universidade Federal do ABC, São Paulo, Brazil*

A. Aleksandrov, G. Antchev, I. Atanasov, R. Hadjiiska, P. Iaydjiev, M. Misheva, M. Rodozov, M. Shopova, G. Sultanov

Institute for Nuclear Research and Nuclear Energy, Bulgarian Academy of Sciences, Sofia, Bulgaria

M. Bonchev, A. Dimitrov, T. Ivanov, L. Litov, B. Pavlov, P. Petkov, A. Petrov

University of Sofia, Sofia, Bulgaria

W. Fang[3], Q. Guo, H. Wang, L. Yuan

Beihang University, Beijing, China

M. Ahmad, Z. Hu, Y. Wang

Department of Physics, Tsinghua University, Beijing, China

E. Chapon, G.M. Chen [9], H.S. Chen [9], M. Chen, C.H. Jiang, D. Leggat, H. Liao, Z. Liu, R. Sharma, A. Spiezia, J. Tao, J. Thomas-wilsker, J. Wang, H. Zhang, S. Zhang [9], J. Zhao

Institute of High Energy Physics, Beijing, China

A. Agapitos, Y. Ban, C. Chen, A. Levin, J. Li, Q. Li, M. Lu, X. Lyu, Y. Mao, S.J. Qian, D. Wang, Q. Wang, J. Xiao

State Key Laboratory of Nuclear Physics and Technology, Peking University, Beijing, China

Z. You

Sun Yat-Sen University, Guangzhou, China

X. Gao [3]

Institute of Modern Physics and Key Laboratory of Nuclear Physics and Ion-beam Application (MOE) – Fudan University, Shanghai, China

M. Xiao

Zhejiang University, Hangzhou, China

C. Avila, A. Cabrera, C. Florez, J. Fraga, A. Sarkar, M.A. Segura Delgado

Universidad de Los Andes, Bogota, Colombia

J. Jaramillo, J. Mejia Guisao, F. Ramirez, J.D. Ruiz Alvarez, C.A. Salazar González, N. Vanegas Arbelaez

Universidad de Antioquia, Medellin, Colombia

D. Giljanovic, N. Godinovic, D. Lelas, I. Puljak, T. Sculac

University of Split, Faculty of Electrical Engineering, Mechanical Engineering and Naval Architecture, Split, Croatia

Z. Antunovic, M. Kovac

University of Split, Faculty of Science, Split, Croatia

V. Brigljevic, D. Ferencek, D. Majumder, B. Mesic, M. Roguljic, A. Starodumov [10], T. Susa

Institute Rudjer Boskovic, Zagreb, Croatia

M.W. Ather, A. Attikis, E. Erodotou, A. Ioannou, G. Kole, M. Kolosova, S. Konstantinou, G. Mavromanolakis, J. Mousa, C. Nicolaou, F. Ptochos, P.A. Razis, H. Rykaczewski, H. Saka, D. Tsiakkouri

University of Cyprus, Nicosia, Cyprus

M. Finger [11], M. Finger Jr. [11], A. Kveton, J. Tomsa

Charles University, Prague, Czech Republic

E. Ayala

Escuela Politecnica Nacional, Quito, Ecuador

E. Carrera Jarrin

Universidad San Francisco de Quito, Quito, Ecuador

E. Salama [12,13]

Academy of Scientific Research and Technology of the Arab Republic of Egypt, Egyptian Network of High Energy Physics, Cairo, Egypt

M.A. Mahmoud, Y. Mohammed [14]

Center for High Energy Physics (CHEP-FU), Fayoum University, El-Fayoum, Egypt

S. Bhowmik, A. Carvalho Antunes De Oliveira, R.K. Dewanjee, K. Ehataht, M. Kadastik, M. Raidal, C. Veelken

National Institute of Chemical Physics and Biophysics, Tallinn, Estonia

P. Eerola, L. Forthomme, H. Kirschenmann, K. Osterberg, M. Voutilainen

Department of Physics, University of Helsinki, Helsinki, Finland

E. Brücken, F. Garcia, J. Havukainen, V. Karimäki, M.S. Kim, R. Kinnunen, T. Lampén, K. Lassila-Perini, S. Laurila, S. Lehti, T. Lindén, H. Siikonen, E. Tuominen, J. Tuominiemi

Helsinki Institute of Physics, Helsinki, Finland

P. Luukka, T. Tuuva

Lappeenranta University of Technology, Lappeenranta, Finland

M. Besancon, F. Couderc, M. Dejardin, D. Denegri, J.L. Faure, F. Ferri, S. Ganjour, A. Givernaud, P. Gras, G. Hamel de Monchenault, P. Jarry, B. Lenzi, E. Locci, J. Malcles, J. Rander, A. Rosowsky, M.Ö. Sahin, A. Savoy-Navarro [15], M. Titov, G.B. Yu

IRFU, CEA, Université Paris-Saclay, Gif-sur-Yvette, France

S. Ahuja, C. Amendola, F. Beaudette, M. Bonanomi, P. Busson, C. Charlot, O. Davignon, B. Diab, G. Falmagne, R. Granier de Cassagnac, I. Kucher, A. Lobanov, C. Martin Perez, M. Nguyen, C. Ochando, P. Paganini, J. Rembser, R. Salerno, J.B. Sauvan, Y. Sirois, A. Zabi, A. Zghiche

Laboratoire Leprince-Ringuet, CNRS/IN2P3, Ecole Polytechnique, Institut Polytechnique de Paris, France

J.-L. Agram [16], J. Andrea, D. Bloch, G. Bourgatte, J.-M. Brom, E.C. Chabert, C. Collard, J.-C. Fontaine [16], D. Gelé, U. Goerlach, C. Grimault, A.-C. Le Bihan, P. Van Hove

Université de Strasbourg, CNRS, IPHC UMR 7178, Strasbourg, France

E. Asilar, S. Beauceron, C. Bernet, G. Boudoul, C. Camen, A. Carle, N. Chanon, D. Contardo, P. Depasse, H. El Mamouni, J. Fay, S. Gascon, M. Gouzevitch, B. Ille, Sa. Jain, I.B. Laktineh, H. Lattaud, A. Lesauvage, M. Lethuillier, L. Mirabito, L. Torterotot, G. Touquet, M. Vander Donckt, S. Viret

Université de Lyon, Université Claude Bernard Lyon 1, CNRS-IN2P3, Institut de Physique Nucléaire de Lyon, Villeurbanne, France

T. Toriashvili [17]

Georgian Technical University, Tbilisi, Georgia

Z. Tsamalaidze [11]

Tbilisi State University, Tbilisi, Georgia

L. Feld, K. Klein, M. Lipinski, D. Meuser, A. Pauls, M. Preuten, M.P. Rauch, J. Schulz, M. Teroerde

RWTH Aachen University, I. Physikalisches Institut, Aachen, Germany

D. Eliseev, M. Erdmann, P. Fackeldey, B. Fischer, S. Ghosh, T. Hebbeker, K. Hoepfner, H. Keller, L. Mastrolorenzo, M. Merschmeyer, A. Meyer, P. Millet, G. Mocellin, S. Mondal, S. Mukherjee, D. Noll, A. Novak, T. Pook, A. Pozdnyakov, T. Quast, M. Radziej, Y. Rath, H. Reithler, J. Roemer, A. Schmidt, S.C. Schuler, A. Sharma, S. Wiedenbeck, S. Zaleski

RWTH Aachen University, III. Physikalisches Institut A, Aachen, Germany

C. Dziwok, G. Flügge, W. Haj Ahmad [18], O. Hlushchenko, T. Kress, A. Nowack, C. Pistone, O. Pooth, D. Roy, H. Sert, A. Stahl [19], T. Ziemons

RWTH Aachen University, III. Physikalisches Institut B, Aachen, Germany

H. Aarup Petersen, M. Aldaya Martin, P. Asmuss, I. Babounikau, S. Baxter, O. Behnke,
A. Bermúdez Martínez, A.A. Bin Anuar, K. Borras [20], V. Botta, D. Brunner, A. Campbell, A. Cardini,
P. Connor, S. Consuegra Rodríguez, V. Danilov, A. De Wit, M.M. Defranchis, L. Didukh,
D. Domínguez Damiani, G. Eckerlin, D. Eckstein, T. Eichhorn, A. Elwood, L.I. Estevez Banos, E. Gallo [21],
A. Geiser, A. Giraldi, A. Grohsjean, M. Guthoff, M. Haranko, A. Harb, A. Jafari [22], N.Z. Jomhari, H. Jung,
A. Kasem [20], M. Kasemann, H. Kaveh, J. Keaveney, C. Kleinwort, J. Knolle, D. Krücker, W. Lange, T. Lenz,
J. Lidrych, K. Lipka, W. Lohmann [23], R. Mankel, I.-A. Melzer-Pellmann, J. Metwally, A.B. Meyer, M. Meyer,
M. Missiroli, J. Mnich, A. Mussgiller, V. Myronenko, Y. Otarid, D. Pérez Adán, S.K. Pflitsch, D. Pitzl,
A. Raspereza, A. Saggio, A. Saibel, M. Savitskyi, V. Scheurer, P. Schütze, C. Schwanenberger,
R. Shevchenko, A. Singh, R.E. Sosa Ricardo, H. Tholen, N. Tonon, O. Turkot, A. Vagnerini,
M. Van De Klundert, R. Walsh, D. Walter, Y. Wen, K. Wichmann, C. Wissing, S. Wuchterl, O. Zenaiev,
R. Zlebcik

Deutsches Elektronen-Synchrotron, Hamburg, Germany

R. Aggleton, S. Bein, L. Benato, A. Benecke, K. De Leo, T. Dreyer, A. Ebrahimi, F. Feindt, A. Fröhlich,
C. Garbers, E. Garutti, D. Gonzalez, P. Gunnellini, J. Haller, A. Hinzmann, A. Karavdina, G. Kasieczka,
R. Klanner, R. Kogler, S. Kurz, V. Kutzner, J. Lange, T. Lange, A. Malara, J. Multhaup, C.E.N. Niemeyer,
A. Nigamova, K.J. Pena Rodriguez, O. Rieger, P. Schleper, S. Schumann, J. Schwandt, D. Schwarz,
J. Sonneveld, H. Stadie, G. Steinbrück, B. Vormwald, I. Zoi

University of Hamburg, Hamburg, Germany

M. Baselga, S. Baur, J. Bechtel, T. Berger, E. Butz, R. Caspart, T. Chwalek, W. De Boer, A. Dierlamm,
A. Droll, K. El Morabit, N. Faltermann, K. Flöh, M. Giffels, A. Gottmann, F. Hartmann [19], C. Heidecker,
U. Husemann, M.A. Iqbal, I. Katkov [24], P. Keicher, R. Koppenhöfer, S. Kudella, S. Maier, M. Metzler,
S. Mitra, M.U. Mozer, D. Müller, Th. Müller, M. Musich, G. Quast, K. Rabbertz, J. Rauser, D. Savoiu,
D. Schäfer, M. Schnepf, M. Schröder, D. Seith, I. Shvetsov, H.J. Simonis, R. Ulrich, M. Wassmer, M. Weber,
C. Wöhrmann, R. Wolf, S. Wozniewski

Karlsruher Institut fuer Technologie, Karlsruhe, Germany

G. Anagnostou, P. Asenov, G. Daskalakis, T. Geralis, A. Kyriakis, D. Loukas, G. Paspalaki, A. Stakia

Institute of Nuclear and Particle Physics (INPP), NCSR Demokritos, Aghia Paraskevi, Greece

M. Diamantopoulou, D. Karasavvas, G. Karathanasis, P. Kontaxakis, C.K. Koraka, A. Manousakis-katsikakis,
A. Panagiotou, I. Papavergou, N. Saoulidou, K. Theofilatos, K. Vellidis, E. Vourliotis

National and Kapodistrian University of Athens, Athens, Greece

G. Bakas, K. Kousouris, I. Papakrivopoulos, G. Tsipolitis, A. Zacharopoulou

National Technical University of Athens, Athens, Greece

I. Evangelou, C. Foudas, P. Gianneios, P. Katsoulis, P. Kokkas, S. Mallios, K. Manitara, N. Manthos,
I. Papadopoulos, J. Strologas

University of Ioánnina, Ioánnina, Greece

M. Bartók [25], R. Chudasama, M. Csanad, M.M.A. Gadallah [26], P. Major, K. Mandal, A. Mehta, G. Pasztor,
O. Surányi, G.I. Veres

MTA-ELTE Lendület CMS Particle and Nuclear Physics Group, Eötvös Loránd University, Budapest, Hungary

G. Bencze, C. Hajdu, D. Horvath [27], F. Sikler, V. Veszpremi, G. Vesztergombi [†]

Wigner Research Centre for Physics, Budapest, Hungary

N. Beni, S. Czellar, J. Karancsi [25], J. Molnar, Z. Szillasi, D. Teyssier

Institute of Nuclear Research ATOMKI, Debrecen, Hungary

P. Raics, Z.L. Trocsanyi, B. Ujvari

Institute of Physics, University of Debrecen, Debrecen, Hungary

T. Csorgo, S. Lökös [28], F. Nemes, T. Novak

Eszterhazy Karoly University, Karoly Robert Campus, Gyongyos, Hungary

S. Choudhury, J.R. Komaragiri, D. Kumar, L. Panwar, P.C. Tiwari

Indian Institute of Science (IISc), Bangalore, India

S. Bahinipati [29], D. Dash, C. Kar, P. Mal, T. Mishra, V.K. Muraleedharan Nair Bindhu, A. Nayak [30], D.K. Sahoo [29], N. Sur, S.K. Swain

National Institute of Science Education and Research, HBNI, Bhubaneswar, India

S. Bansal, S.B. Beri, V. Bhatnagar, S. Chauhan, N. Dhingra [31], R. Gupta, A. Kaur, A. Kaur, M. Kaur, S. Kaur, P. Kumari, M. Lohan, M. Meena, K. Sandeep, S. Sharma, J.B. Singh, A.K. Virdi

Panjab University, Chandigarh, India

A. Ahmed, A. Bhardwaj, B.C. Choudhary, R.B. Garg, M. Gola, S. Keshri, A. Kumar, M. Naimuddin, P. Priyanka, K. Ranjan, A. Shah

University of Delhi, Delhi, India

M. Bharti [32], R. Bhattacharya, S. Bhattacharya, D. Bhowmik, S. Dutta, S. Ghosh, B. Gomber [33], M. Maity [34], S. Nandan, P. Palit, A. Purohit, P.K. Rout, G. Saha, S. Sarkar, M. Sharan, B. Singh [32], S. Thakur [32]

Saha Institute of Nuclear Physics, HBNI, Kolkata, India

P.K. Behera, S.C. Behera, P. Kalbhor, A. Muhammad, R. Pradhan, P.R. Pujahari, A. Sharma, A.K. Sikdar

Indian Institute of Technology Madras, Madras, India

D. Dutta, V. Jha, V. Kumar, D.K. Mishra, K. Naskar [35], P.K. Netrakanti, L.M. Pant, P. Shukla

Bhabha Atomic Research Centre, Mumbai, India

T. Aziz, M.A. Bhat, S. Dugad, R. Kumar Verma, U. Sarkar

Tata Institute of Fundamental Research-A, Mumbai, India

S. Banerjee, S. Bhattacharya, S. Chatterjee, P. Das, M. Guchait, S. Karmakar, S. Kumar, G. Majumder, K. Mazumdar, S. Mukherjee, D. Roy, N. Sahoo

Tata Institute of Fundamental Research-B, Mumbai, India

S. Dube, B. Kansal, A. Kapoor, K. Kothekar, S. Pandey, A. Rane, A. Rastogi, S. Sharma

Indian Institute of Science Education and Research (IISER), Pune, India

H. Bakhshiansohi [36]

Isfahan University of Technology, Isfahan, Iran

S. Chenarani [37], S.M. Etesami, M. Khakzad, M. Mohammadi Najafabadi, M. Naseri

Institute for Research in Fundamental Sciences (IPM), Tehran, Iran

M. Felcini, M. Grunewald

University College Dublin, Dublin, Ireland

M. Abbrescia [a,b], R. Aly [a,b,38], C. Aruta [a,b], A. Colaleo [a], D. Creanza [a,c], N. De Filippis [a,c], M. De Palma [a,b], A. Di Florio [a,b], A. Di Pilato [a,b], W. Elmetenawee [a,b], L. Fiore [a], A. Gelmi [a,b], M. Gul [a], G. Iaselli [a,c], M. Ince [a,b], S. Lezki [a,b], G. Maggi [a,c], M. Maggi [a], I. Margjeka [a,b], J.A. Merlin [a], S. My [a,b], S. Nuzzo [a,b], A. Pompili [a,b], G. Pugliese [a,c], A. Ranieri [a], G. Selvaggi [a,b], L. Silvestris [a], F.M. Simone [a,b], R. Venditti [a], P. Verwilligen [a]

a *INFN Sezione di Bari, Bari, Italy*
b *Università di Bari, Bari, Italy*
c *Politecnico di Bari, Bari, Italy*

G. Abbiendi [a], C. Battilana [a,b], D. Bonacorsi [a,b], L. Borgonovi [a,b], S. Braibant-Giacomelli [a,b], R. Campanini [a,b], P. Capiluppi [a,b], A. Castro [a,b], F.R. Cavallo [a], C. Ciocca [a], M. Cuffiani [a,b], G.M. Dallavalle [a], T. Diotalevi [a,b], F. Fabbri [a], A. Fanfani [a,b], E. Fontanesi [a,b], P. Giacomelli [a], C. Grandi [a], L. Guiducci [a,b], F. Iemmi [a,b], S. Lo Meo [a,39], S. Marcellini [a], G. Masetti [a], F.L. Navarria [a,b], A. Perrotta [a], F. Primavera [a,b], A.M. Rossi [a,b], T. Rovelli [a,b], G.P. Siroli [a,b], N. Tosi [a]

a *INFN Sezione di Bologna, Bologna, Italy*
b *Università di Bologna, Bologna, Italy*

S. Albergo [a,b,40], S. Costa [a,b], A. Di Mattia [a], R. Potenza [a,b], A. Tricomi [a,b,40], C. Tuve [a,b]

a *INFN Sezione di Catania, Catania, Italy*
b *Università di Catania, Catania, Italy*

G. Barbagli [a], A. Cassese [a], R. Ceccarelli [a,b], V. Ciulli [a,b], C. Civinini [a], R. D'Alessandro [a,b], F. Fiori [a], E. Focardi [a,b], G. Latino [a,b], P. Lenzi [a,b], M. Lizzo [a,b], M. Meschini [a], S. Paoletti [a], R. Seidita [a,b], G. Sguazzoni [a], L. Viliani [a]

a *INFN Sezione di Firenze, Firenze, Italy*
b *Università di Firenze, Firenze, Italy*

L. Benussi, S. Bianco, D. Piccolo

INFN Laboratori Nazionali di Frascati, Frascati, Italy

M. Bozzo [a,b], F. Ferro [a], R. Mulargia [a,b], E. Robutti [a], S. Tosi [a,b]

a *INFN Sezione di Genova, Genova, Italy*
b *Università di Genova, Genova, Italy*

A. Benaglia [a], A. Beschi [a,b], F. Brivio [a,b], F. Cetorelli [a,b], V. Ciriolo [a,b,19], F. De Guio [a,b], M.E. Dinardo [a,b], P. Dini [a], S. Gennai [a], A. Ghezzi [a,b], P. Govoni [a,b], L. Guzzi [a,b], M. Malberti [a], S. Malvezzi [a], D. Menasce [a], F. Monti [a,b], L. Moroni [a], M. Paganoni [a,b], D. Pedrini [a], S. Ragazzi [a,b], T. Tabarelli de Fatis [a,b], D. Valsecchi [a,b,19], D. Zuolo [a,b]

a *INFN Sezione di Milano-Bicocca, Milano, Italy*
b *Università di Milano-Bicocca, Milano, Italy*

S. Buontempo [a], N. Cavallo [a,c], A. De Iorio [a,b], F. Fabozzi [a,c], F. Fienga [a], A.O.M. Iorio [a,b], L. Layer [a,b], L. Lista [a,b], S. Meola [a,d,19], P. Paolucci [a,19], B. Rossi [a], C. Sciacca [a,b], E. Voevodina [a,b]

a *INFN Sezione di Napoli, Napoli, Italy*
b *Università di Napoli 'Federico II', Napoli, Italy*
c *Università della Basilicata, Potenza, Italy*
d *Università G. Marconi, Roma, Italy*

P. Azzi [a], N. Bacchetta [a], D. Bisello [a,b], A. Boletti [a,b], A. Bragagnolo [a,b], R. Carlin [a,b], P. Checchia [a], P. De Castro Manzano [a], T. Dorigo [a], U. Dosselli [a], F. Gasparini [a,b], U. Gasparini [a,b], S.Y. Hoh [a,b],

M. Margoni [a,b], A.T. Meneguzzo [a,b], M. Presilla [b], P. Ronchese [a,b], R. Rossin [a,b], F. Simonetto [a,b], G. Strong [a], A. Tiko [a], M. Tosi [a,b], M. Zanetti [a,b], P. Zotto [a,b], A. Zucchetta [a,b], G. Zumerle [a,b]

[a] *INFN Sezione di Padova, Padova, Italy*
[b] *Università di Padova, Padova, Italy*

A. Braghieri [a], S. Calzaferri [a,b], D. Fiorina [a,b], P. Montagna [a,b], S.P. Ratti [a,b], V. Re [a], M. Ressegotti [a,b], C. Riccardi [a,b], P. Salvini [a], I. Vai [a], P. Vitulo [a,b]

[a] *INFN Sezione di Pavia, Pavia, Italy*
[b] *Università di Pavia, Pavia, Italy*

M. Biasini [a,b], G.M. Bilei [a], D. Ciangottini [a,b], L. Fanò [a,b], P. Lariccia [a,b], G. Mantovani [a,b], V. Mariani [a,b], M. Menichelli [a], F. Moscatelli [a], A. Rossi [a,b], A. Santocchia [a,b], D. Spiga [a], T. Tedeschi [a,b]

[a] *INFN Sezione di Perugia, Perugia, Italy*
[b] *Università di Perugia, Perugia, Italy*

K. Androsov [a], P. Azzurri [a], G. Bagliesi [a], V. Bertacchi [a,c], L. Bianchini [a], T. Boccali [a], R. Castaldi [a], M.A. Ciocci [a,b], R. Dell'Orso [a], M.R. Di Domenico [a,b], S. Donato [a], L. Giannini [a,c], A. Giassi [a], M.T. Grippo [a], F. Ligabue [a,c], E. Manca [a,c], G. Mandorli [a,c], A. Messineo [a,b], F. Palla [a], G. Ramirez-Sanchez [a,c], A. Rizzi [a,b], G. Rolandi [a,c], S. Roy Chowdhury [a,c], A. Scribano [a], N. Shafiei [a,b], P. Spagnolo [a], R. Tenchini [a], G. Tonelli [a,b], N. Turini [a], A. Venturi [a], P.G. Verdini [a]

[a] *INFN Sezione di Pisa, Pisa, Italy*
[b] *Università di Pisa, Pisa, Italy*
[c] *Scuola Normale Superiore di Pisa, Pisa, Italy*

F. Cavallari [a], M. Cipriani [a,b], D. Del Re [a,b], E. Di Marco [a], M. Diemoz [a], E. Longo [a,b], P. Meridiani [a], G. Organtini [a,b], F. Pandolfi [a], R. Paramatti [a,b], C. Quaranta [a,b], S. Rahatlou [a,b], C. Rovelli [a], F. Santanastasio [a,b], L. Soffi [a,b], R. Tramontano [a,b]

[a] *INFN Sezione di Roma, Rome, Italy*
[b] *Sapienza Università di Roma, Rome, Italy*

N. Amapane [a,b], R. Arcidiacono [a,c], S. Argiro [a,b], M. Arneodo [a,c], N. Bartosik [a], R. Bellan [a,b], A. Bellora [a,b], C. Biino [a], A. Cappati [a,b], N. Cartiglia [a], S. Cometti [a], M. Costa [a,b], R. Covarelli [a,b], N. Demaria [a], B. Kiani [a,b], F. Legger [a], C. Mariotti [a], S. Maselli [a], E. Migliore [a,b], V. Monaco [a,b], E. Monteil [a,b], M. Monteno [a], M.M. Obertino [a,b], G. Ortona [a], L. Pacher [a,b], N. Pastrone [a], M. Pelliccioni [a], G.L. Pinna Angioni [a,b], M. Ruspa [a,c], R. Salvatico [a,b], F. Siviero [a,b], V. Sola [a], A. Solano [a,b], D. Soldi [a,b], A. Staiano [a], D. Trocino [a,b]

[a] *INFN Sezione di Torino, Torino, Italy*
[b] *Università di Torino, Torino, Italy*
[c] *Università del Piemonte Orientale, Novara, Italy*

S. Belforte [a], V. Candelise [a,b], M. Casarsa [a], F. Cossutti [a], A. Da Rold [a,b], G. Della Ricca [a,b], F. Vazzoler [a,b]

[a] *INFN Sezione di Trieste, Trieste, Italy*
[b] *Università di Trieste, Trieste, Italy*

S. Dogra, C. Huh, B. Kim, D.H. Kim, G.N. Kim, J. Lee, S.W. Lee, C.S. Moon, Y.D. Oh, S.I. Pak, S. Sekmen, Y.C. Yang

Kyungpook National University, Daegu, Republic of Korea

H. Kim, D.H. Moon

Chonnam National University, Institute for Universe and Elementary Particles, Kwangju, Republic of Korea

B. Francois, T.J. Kim, J. Park

Hanyang University, Seoul, Republic of Korea

S. Cho, S. Choi, Y. Go, S. Ha, B. Hong, K. Lee, K.S. Lee, J. Lim, J. Park, S.K. Park, J. Yoo

Korea University, Seoul, Republic of Korea

J. Goh, A. Gurtu

Kyung Hee University, Department of Physics, Seoul, Republic of Korea

H.S. Kim, Y. Kim

Sejong University, Seoul, Republic of Korea

J. Almond, J.H. Bhyun, J. Choi, S. Jeon, J. Kim, J.S. Kim, S. Ko, H. Kwon, H. Lee, K. Lee, S. Lee, K. Nam, B.H. Oh, M. Oh, S.B. Oh, B.C. Radburn-Smith, H. Seo, U.K. Yang, I. Yoon

Seoul National University, Seoul, Republic of Korea

D. Jeon, J.H. Kim, B. Ko, J.S.H. Lee, I.C. Park, Y. Roh, D. Song, I.J. Watson

University of Seoul, Seoul, Republic of Korea

H.D. Yoo

Yonsei University, Department of Physics, Seoul, Republic of Korea

Y. Choi, C. Hwang, Y. Jeong, H. Lee, J. Lee, Y. Lee, I. Yu

Sungkyunkwan University, Suwon, Republic of Korea

V. Veckalns [41]

Riga Technical University, Riga, Latvia

A. Juodagalvis, A. Rinkevicius, G. Tamulaitis

Vilnius University, Vilnius, Lithuania

W.A.T. Wan Abdullah, M.N. Yusli, Z. Zolkapli

National Centre for Particle Physics, Universiti Malaya, Kuala Lumpur, Malaysia

J.F. Benitez, A. Castaneda Hernandez, J.A. Murillo Quijada, L. Valencia Palomo

Universidad de Sonora (UNISON), Hermosillo, Mexico

H. Castilla-Valdez, E. De La Cruz-Burelo, I. Heredia-De La Cruz [42], R. Lopez-Fernandez, A. Sanchez-Hernandez

Centro de Investigacion y de Estudios Avanzados del IPN, Mexico City, Mexico

S. Carrillo Moreno, C. Oropeza Barrera, M. Ramirez-Garcia, F. Vazquez Valencia

Universidad Iberoamericana, Mexico City, Mexico

J. Eysermans, I. Pedraza, H.A. Salazar Ibarguen, C. Uribe Estrada

Benemerita Universidad Autonoma de Puebla, Puebla, Mexico

A. Morelos Pineda

Universidad Autónoma de San Luis Potosí, San Luis Potosí, Mexico

J. Mijuskovic [4], N. Raicevic

University of Montenegro, Podgorica, Montenegro

D. Krofcheck

University of Auckland, Auckland, New Zealand

S. Bheesette, P.H. Butler

University of Canterbury, Christchurch, New Zealand

A. Ahmad, M.I. Asghar, M.I.M. Awan, Q. Hassan, H.R. Hoorani, W.A. Khan, M.A. Shah, M. Shoaib,
M. Waqas

National Centre for Physics, Quaid-I-Azam University, Islamabad, Pakistan

V. Avati, L. Grzanka, M. Malawski

AGH University of Science and Technology Faculty of Computer Science, Electronics and Telecommunications, Krakow, Poland

H. Bialkowska, M. Bluj, B. Boimska, T. Frueboes, M. Górski, M. Kazana, M. Szleper, P. Traczyk, P. Zalewski

National Centre for Nuclear Research, Swierk, Poland

K. Bunkowski, A. Byszuk [43], K. Doroba, A. Kalinowski, M. Konecki, J. Krolikowski, M. Olszewski,
M. Walczak

Institute of Experimental Physics, Faculty of Physics, University of Warsaw, Warsaw, Poland

M. Araujo, P. Bargassa, D. Bastos, A. Di Francesco, P. Faccioli, B. Galinhas, M. Gallinaro, J. Hollar,
N. Leonardo, T. Niknejad, J. Seixas, K. Shchelina, O. Toldaiev, J. Varela

Laboratório de Instrumentação e Física Experimental de Partículas, Lisboa, Portugal

S. Afanasiev, P. Bunin, M. Gavrilenko, I. Golutvin, I. Gorbunov, A. Kamenev, V. Karjavine, A. Lanev,
A. Malakhov, V. Matveev [44,45], P. Moisenz, V. Palichik, V. Perelygin, M. Savina, D. Seitova, V. Shalaev,
S. Shmatov, S. Shulha, V. Smirnov, O. Teryaev, N. Voytishin, A. Zarubin, I. Zhizhin

Joint Institute for Nuclear Research, Dubna, Russia

G. Gavrilov, V. Golovtcov, Y. Ivanov, V. Kim [46], E. Kuznetsova [47], V. Murzin, V. Oreshkin, I. Smirnov,
D. Sosnov, V. Sulimov, L. Uvarov, S. Volkov, A. Vorobyev

Petersburg Nuclear Physics Institute, Gatchina (St. Petersburg), Russia

Yu. Andreev, A. Dermenev, S. Gninenko, N. Golubev, A. Karneyeu, M. Kirsanov, N. Krasnikov,
A. Pashenkov, G. Pivovarov, D. Tlisov, A. Toropin

Institute for Nuclear Research, Moscow, Russia

V. Epshteyn, V. Gavrilov, N. Lychkovskaya, A. Nikitenko [48], V. Popov, I. Pozdnyakov, G. Safronov,
A. Spiridonov, A. Stepennov, M. Toms, E. Vlasov, A. Zhokin

Institute for Theoretical and Experimental Physics named by A.I. Alikhanov of NRC 'Kurchatov Institute', Moscow, Russia

T. Aushev

Moscow Institute of Physics and Technology, Moscow, Russia

R. Chistov [49], M. Danilov [49], A. Oskin, P. Parygin, V. Rusinov

National Research Nuclear University 'Moscow Engineering Physics Institute' (MEPhI), Moscow, Russia

V. Andreev, M. Azarkin, I. Dremin, M. Kirakosyan, A. Terkulov

P.N. Lebedev Physical Institute, Moscow, Russia

A. Belyaev, E. Boos, M. Dubinin [50], L. Dudko, A. Ershov, A. Gribushin, V. Klyukhin, O. Kodolova, I. Lokhtin, S. Obraztsov, S. Petrushanko, V. Savrin, A. Snigirev

Skobeltsyn Institute of Nuclear Physics, Lomonosov Moscow State University, Moscow, Russia

V. Blinov [51], T. Dimova [51], L. Kardapoltsev [51], I. Ovtin [51], Y. Skovpen [51]

Novosibirsk State University (NSU), Novosibirsk, Russia

I. Azhgirey, I. Bayshev, V. Kachanov, A. Kalinin, D. Konstantinov, V. Petrov, R. Ryutin, A. Sobol, S. Troshin, N. Tyurin, A. Uzunian, A. Volkov

Institute for High Energy Physics of National Research Centre 'Kurchatov Institute', Protvino, Russia

A. Babaev, A. Iuzhakov, V. Okhotnikov, L. Sukhikh

National Research Tomsk Polytechnic University, Tomsk, Russia

V. Borchsh, V. Ivanchenko, E. Tcherniaev

Tomsk State University, Tomsk, Russia

P. Adzic [52], P. Cirkovic, M. Dordevic, P. Milenovic, J. Milosevic

University of Belgrade: Faculty of Physics and VINCA Institute of Nuclear Sciences, Serbia

M. Aguilar-Benitez, J. Alcaraz Maestre, A. Álvarez Fernández, I. Bachiller, M. Barrio Luna, Cristina Fernandez Bedoya, J.A. Brochero Cifuentes, C.A. Carrillo Montoya, M. Cepeda, M. Cerrada, N. Colino, B. De La Cruz, A. Delgado Peris, J.P. Fernández Ramos, J. Flix, M.C. Fouz, O. Gonzalez Lopez, S. Goy Lopez, J.M. Hernandez, M.I. Josa, D. Moran, Á. Navarro Tobar, A. Pérez-Calero Yzquierdo, J. Puerta Pelayo, I. Redondo, L. Romero, S. Sánchez Navas, M.S. Soares, A. Triossi, C. Willmott

Centro de Investigaciones Energéticas Medioambientales y Tecnológicas (CIEMAT), Madrid, Spain

C. Albajar, J.F. de Trocóniz, R. Reyes-Almanza

Universidad Autónoma de Madrid, Madrid, Spain

B. Alvarez Gonzalez, J. Cuevas, C. Erice, J. Fernandez Menendez, S. Folgueras, I. Gonzalez Caballero, E. Palencia Cortezon, C. Ramón Álvarez, V. Rodríguez Bouza, S. Sanchez Cruz

Universidad de Oviedo, Instituto Universitario de Ciencias y Tecnologías Espaciales de Asturias (ICTEA), Oviedo, Spain

I.J. Cabrillo, A. Calderon, B. Chazin Quero, J. Duarte Campderros, M. Fernandez, P.J. Fernández Manteca, A. García Alonso, G. Gomez, C. Martinez Rivero, P. Martinez Ruiz del Arbol, F. Matorras, J. Piedra Gomez, C. Prieels, F. Ricci-Tam, T. Rodrigo, A. Ruiz-Jimeno, L. Russo [53], L. Scodellaro, I. Vila, J.M. Vizan Garcia

Instituto de Física de Cantabria (IFCA), CSIC-Universidad de Cantabria, Santander, Spain

M.K. Jayananda, B. Kailasapathy [54], D.U.J. Sonnadara, D.D.C. Wickramarathna

University of Colombo, Colombo, Sri Lanka

W.G.D. Dharmaratna, K. Liyanage, N. Perera, N. Wickramage

University of Ruhuna, Department of Physics, Matara, Sri Lanka

T.K. Aarrestad, D. Abbaneo, B. Akgun, E. Auffray, G. Auzinger, J. Baechler, P. Baillon, A.H. Ball, D. Barney, J. Bendavid, M. Bianco, A. Bocci, P. Bortignon, E. Bossini, E. Brondolin, T. Camporesi, G. Cerminara, L. Cristella, D. d'Enterria, A. Dabrowski, N. Daci, V. Daponte, A. David, A. De Roeck, M. Deile, R. Di Maria, M. Dobson, M. Dünser, N. Dupont, A. Elliott-Peisert, N. Emriskova, F. Fallavollita [55], D. Fasanella, S. Fiorendi, G. Franzoni, J. Fulcher, W. Funk, S. Giani, D. Gigi, K. Gill, F. Glege, L. Gouskos, M. Gruchala, M. Guilbaud, D. Gulhan, J. Hegeman, Y. Iiyama, V. Innocente, T. James, P. Janot, J. Kaspar, J. Kieseler,

M. Komm, N. Kratochwil, C. Lange, P. Lecoq, K. Long, C. Lourenço, L. Malgeri, M. Mannelli, A. Massironi, F. Meijers, S. Mersi, E. Meschi, F. Moortgat, M. Mulders, J. Ngadiuba, J. Niedziela, S. Orfanelli, L. Orsini, F. Pantaleo [19], L. Pape, E. Perez, M. Peruzzi, A. Petrilli, G. Petrucciani, A. Pfeiffer, M. Pierini, D. Rabady, A. Racz, M. Rieger, M. Rovere, H. Sakulin, J. Salfeld-Nebgen, S. Scarfi, C. Schäfer, C. Schwick, M. Selvaggi, A. Sharma, P. Silva, W. Snoeys, P. Sphicas [56], J. Steggemann, S. Summers, V.R. Tavolaro, D. Treille, A. Tsirou, G.P. Van Onsem, A. Vartak, M. Verzetti, K.A. Wozniak, W.D. Zeuner

CERN, European Organization for Nuclear Research, Geneva, Switzerland

L. Caminada [57], W. Erdmann, R. Horisberger, Q. Ingram, H.C. Kaestli, D. Kotlinski, U. Langenegger, T. Rohe

Paul Scherrer Institut, Villigen, Switzerland

M. Backhaus, P. Berger, A. Calandri, N. Chernyavskaya, G. Dissertori, M. Dittmar, M. Donegà, C. Dorfer, T. Gadek, T.A. Gómez Espinosa, C. Grab, D. Hits, W. Lustermann, A.-M. Lyon, R.A. Manzoni, M.T. Meinhard, F. Micheli, P. Musella, F. Nessi-Tedaldi, F. Pauss, V. Perovic, G. Perrin, L. Perrozzi, S. Pigazzini, M.G. Ratti, M. Reichmann, C. Reissel, T. Reitenspiess, B. Ristic, D. Ruini, D.A. Sanz Becerra, M. Schönenberger, L. Shchutska, V. Stampf, M.L. Vesterbacka Olsson, R. Wallny, D.H. Zhu

ETH Zurich – Institute for Particle Physics and Astrophysics (IPA), Zurich, Switzerland

C. Amsler [58], C. Botta, D. Brzhechko, M.F. Canelli, A. De Cosa, R. Del Burgo, J.K. Heikkilä, M. Huwiler, A. Jofrehei, B. Kilminster, S. Leontsinis, A. Macchiolo, P. Meiring, V.M. Mikuni, U. Molinatti, I. Neutelings, G. Rauco, A. Reimers, P. Robmann, K. Schweiger, Y. Takahashi, S. Wertz

Universität Zürich, Zurich, Switzerland

C. Adloff [59], C.M. Kuo, W. Lin, A. Roy, T. Sarkar [34], S.S. Yu

National Central University, Chung-Li, Taiwan

L. Ceard, P. Chang, Y. Chao, K.F. Chen, P.H. Chen, W.-S. Hou, Y.y. Li, R.-S. Lu, E. Paganis, A. Psallidas, A. Steen, E. Yazgan

National Taiwan University (NTU), Taipei, Taiwan

B. Asavapibhop, C. Asawatangtrakuldee, N. Srimanobhas

Chulalongkorn University, Faculty of Science, Department of Physics, Bangkok, Thailand

F. Boran, S. Damarseckin [60], Z.S. Demiroglu, F. Dolek, C. Dozen [61], I. Dumanoglu [62], E. Eskut, G. Gokbulut, Y. Guler, E. Gurpinar Guler [63], I. Hos [64], C. Isik, E.E. Kangal [65], O. Kara, A. Kayis Topaksu, U. Kiminsu, G. Onengut, K. Ozdemir [66], A. Polatoz, A.E. Simsek, B. Tali [67], U.G. Tok, S. Turkcapar, I.S. Zorbakir, C. Zorbilmez

Çukurova University, Physics Department, Science and Art Faculty, Adana, Turkey

B. Isildak [68], G. Karapinar [69], K. Ocalan [70], M. Yalvac [71]

Middle East Technical University, Physics Department, Ankara, Turkey

I.O. Atakisi, E. Gülmez, M. Kaya [72], O. Kaya [73], Ö. Özçelik, S. Tekten [74], E.A. Yetkin [75]

Bogazici University, Istanbul, Turkey

A. Cakir, K. Cankocak [62], Y. Komurcu, S. Sen [76]

Istanbul Technical University, Istanbul, Turkey

F. Aydogmus Sen, S. Cerci [67], B. Kaynak, S. Ozkorucuklu, D. Sunar Cerci [67]

Istanbul University, Istanbul, Turkey

B. Grynyov

Institute for Scintillation Materials of National Academy of Science of Ukraine, Kharkov, Ukraine

L. Levchuk

National Scientific Center, Kharkov Institute of Physics and Technology, Kharkov, Ukraine

E. Bhal, S. Bologna, J.J. Brooke, D. Burns [77], E. Clement, D. Cussans, H. Flacher, J. Goldstein, G.P. Heath, H.F. Heath, L. Kreczko, B. Krikler, S. Paramesvaran, T. Sakuma, S. Seif El Nasr-Storey, V.J. Smith, J. Taylor, A. Titterton

University of Bristol, Bristol, United Kingdom

K.W. Bell, A. Belyaev [78], C. Brew, R.M. Brown, D.J.A. Cockerill, K.V. Ellis, K. Harder, S. Harper, J. Linacre, K. Manolopoulos, D.M. Newbold, E. Olaiya, D. Petyt, T. Reis, T. Schuh, C.H. Shepherd-Themistocleous, A. Thea, I.R. Tomalin, T. Williams

Rutherford Appleton Laboratory, Didcot, United Kingdom

R. Bainbridge, P. Bloch, S. Bonomally, J. Borg, S. Breeze, O. Buchmuller, A. Bundock, V. Cepaitis, G.S. Chahal [79], D. Colling, P. Dauncey, G. Davies, M. Della Negra, P. Everaerts, G. Fedi, G. Hall, G. Iles, J. Langford, L. Lyons, A.-M. Magnan, S. Malik, A. Martelli, V. Milosevic, J. Nash [80], V. Palladino, M. Pesaresi, D.M. Raymond, A. Richards, A. Rose, E. Scott, C. Seez, A. Shtipliyski, M. Stoye, A. Tapper, K. Uchida, T. Virdee [19], N. Wardle, S.N. Webb, D. Winterbottom, A.G. Zecchinelli, S.C. Zenz

Imperial College, London, United Kingdom

J.E. Cole, P.R. Hobson, A. Khan, P. Kyberd, C.K. Mackay, I.D. Reid, L. Teodorescu, S. Zahid

Brunel University, Uxbridge, United Kingdom

A. Brinkerhoff, K. Call, B. Caraway, J. Dittmann, K. Hatakeyama, A.R. Kanuganti, C. Madrid, B. McMaster, N. Pastika, S. Sawant, C. Smith

Baylor University, Waco, USA

R. Bartek, A. Dominguez, R. Uniyal, A.M. Vargas Hernandez

Catholic University of America, Washington, DC, USA

A. Buccilli, O. Charaf, S.I. Cooper, S.V. Gleyzer, C. Henderson, P. Rumerio, C. West

The University of Alabama, Tuscaloosa, USA

A. Akpinar, A. Albert, D. Arcaro, C. Cosby, Z. Demiragli, D. Gastler, C. Richardson, J. Rohlf, K. Salyer, D. Sperka, D. Spitzbart, I. Suarez, S. Yuan, D. Zou

Boston University, Boston, USA

G. Benelli, B. Burkle, X. Coubez [20], D. Cutts, Y.t. Duh, M. Hadley, U. Heintz, J.M. Hogan [81], K.H.M. Kwok, E. Laird, G. Landsberg, K.T. Lau, J. Lee, M. Narain, S. Sagir [82], R. Syarif, E. Usai, W.Y. Wong, D. Yu, W. Zhang

Brown University, Providence, USA

R. Band, C. Brainerd, R. Breedon, M. Calderon De La Barca Sanchez, M. Chertok, J. Conway, R. Conway, P.T. Cox, R. Erbacher, C. Flores, G. Funk, F. Jensen, W. Ko [†], O. Kukral, R. Lander, M. Mulhearn, D. Pellett, J. Pilot, M. Shi, D. Taylor, K. Tos, M. Tripathi, Y. Yao, F. Zhang

University of California, Davis, Davis, USA

M. Bachtis, C. Bravo, R. Cousins, A. Dasgupta, A. Florent, D. Hamilton, J. Hauser, M. Ignatenko, T. Lam, N. Mccoll, W.A. Nash, S. Regnard, D. Saltzberg, C. Schnaible, B. Stone, V. Valuev

University of California, Los Angeles, USA

K. Burt, Y. Chen, R. Clare, J.W. Gary, S.M.A. Ghiasi Shirazi, G. Hanson, G. Karapostoli, O.R. Long, N. Manganelli, M. Olmedo Negrete, M.I. Paneva, W. Si, S. Wimpenny, Y. Zhang

University of California, Riverside, Riverside, USA

J.G. Branson, P. Chang, S. Cittolin, S. Cooperstein, N. Deelen, M. Derdzinski, J. Duarte, R. Gerosa, D. Gilbert, B. Hashemi, D. Klein, V. Krutelyov, J. Letts, M. Masciovecchio, S. May, S. Padhi, M. Pieri, V. Sharma, M. Tadel, F. Würthwein, A. Yagil

University of California, San Diego, La Jolla, USA

N. Amin, R. Bhandari, C. Campagnari, M. Citron, A. Dorsett, V. Dutta, J. Incandela, B. Marsh, H. Mei, A. Ovcharova, H. Qu, M. Quinnan, J. Richman, U. Sarica, D. Stuart, S. Wang

University of California, Santa Barbara – Department of Physics, Santa Barbara, USA

D. Anderson, A. Bornheim, O. Cerri, I. Dutta, J.M. Lawhorn, N. Lu, J. Mao, H.B. Newman, T.Q. Nguyen, J. Pata, M. Spiropulu, J.R. Vlimant, S. Xie, Z. Zhang, R.Y. Zhu

California Institute of Technology, Pasadena, USA

J. Alison, M.B. Andrews, T. Ferguson, T. Mudholkar, M. Paulini, M. Sun, I. Vorobiev, M. Weinberg

Carnegie Mellon University, Pittsburgh, USA

J.P. Cumalat, W.T. Ford, E. MacDonald, T. Mulholland, R. Patel, A. Perloff, K. Stenson, K.A. Ulmer, S.R. Wagner

University of Colorado Boulder, Boulder, USA

J. Alexander, Y. Cheng, J. Chu, D.J. Cranshaw, A. Datta, A. Frankenthal, K. Mcdermott, J. Monroy, J.R. Patterson, D. Quach, A. Ryd, W. Sun, S.M. Tan, Z. Tao, J. Thom, P. Wittich, M. Zientek

Cornell University, Ithaca, USA

S. Abdullin, M. Albrow, M. Alyari, G. Apollinari, A. Apresyan, A. Apyan, S. Banerjee, L.A.T. Bauerdick, A. Beretvas, D. Berry, J. Berryhill, P.C. Bhat, K. Burkett, J.N. Butler, A. Canepa, G.B. Cerati, H.W.K. Cheung, F. Chlebana, M. Cremonesi, V.D. Elvira, J. Freeman, Z. Gecse, E. Gottschalk, L. Gray, D. Green, S. Grünendahl, O. Gutsche, R.M. Harris, S. Hasegawa, R. Heller, T.C. Herwig, J. Hirschauer, B. Jayatilaka, S. Jindariani, M. Johnson, U. Joshi, T. Klijnsma, B. Klima, M.J. Kortelainen, S. Lammel, J. Lewis, D. Lincoln, R. Lipton, M. Liu, T. Liu, J. Lykken, K. Maeshima, D. Mason, P. McBride, P. Merkel, S. Mrenna, S. Nahn, V. O'Dell, V. Papadimitriou, K. Pedro, C. Pena [50], O. Prokofyev, F. Ravera, A. Reinsvold Hall, L. Ristori, B. Schneider, E. Sexton-Kennedy, N. Smith, A. Soha, W.J. Spalding, L. Spiegel, S. Stoynev, J. Strait, L. Taylor, S. Tkaczyk, N.V. Tran, L. Uplegger, E.W. Vaandering, M. Wang, H.A. Weber, A. Woodard

Fermi National Accelerator Laboratory, Batavia, USA

D. Acosta, P. Avery, D. Bourilkov, L. Cadamuro, V. Cherepanov, F. Errico, R.D. Field, D. Guerrero, B.M. Joshi, M. Kim, J. Konigsberg, A. Korytov, K.H. Lo, K. Matchev, N. Menendez, G. Mitselmakher, D. Rosenzweig, K. Shi, J. Wang, S. Wang, X. Zuo

University of Florida, Gainesville, USA

Y.R. Joshi

Florida International University, Miami, USA

T. Adams, A. Askew, D. Diaz, R. Habibullah, S. Hagopian, V. Hagopian, K.F. Johnson, R. Khurana, T. Kolberg, G. Martinez, H. Prosper, C. Schiber, R. Yohay, J. Zhang

Florida State University, Tallahassee, USA

M.M. Baarmand, S. Butalla, T. Elkafrawy [13], M. Hohlmann, D. Noonan, M. Rahmani, M. Saunders, F. Yumiceva

Florida Institute of Technology, Melbourne, USA

M.R. Adams, L. Apanasevich, H. Becerril Gonzalez, R. Cavanaugh, X. Chen, S. Dittmer, O. Evdokimov, C.E. Gerber, D.A. Hangal, D.J. Hofman, C. Mills, G. Oh, T. Roy, M.B. Tonjes, N. Varelas, J. Viinikainen, H. Wang, X. Wang, Z. Wu

University of Illinois at Chicago (UIC), Chicago, USA

M. Alhusseini, B. Bilki [63], K. Dilsiz [83], S. Durgut, R.P. Gandrajula, M. Haytmyradov, V. Khristenko, O.K. Köseyan, J.-P. Merlo, A. Mestvirishvili [84], A. Moeller, J. Nachtman, H. Ogul [85], Y. Onel, F. Ozok [86], A. Penzo, C. Snyder, E. Tiras, J. Wetzel, K. Yi [87]

The University of Iowa, Iowa City, USA

O. Amram, B. Blumenfeld, L. Corcodilos, M. Eminizer, A.V. Gritsan, S. Kyriacou, P. Maksimovic, C. Mantilla, J. Roskes, M. Swartz, T.Á. Vámi

Johns Hopkins University, Baltimore, USA

C. Baldenegro Barrera, P. Baringer, A. Bean, A. Bylinkin, T. Isidori, S. Khalil, J. King, G. Krintiras, A. Kropivnitskaya, C. Lindsey, N. Minafra, M. Murray, C. Rogan, C. Royon, S. Sanders, E. Schmitz, J.D. Tapia Takaki, Q. Wang, J. Williams, G. Wilson

The University of Kansas, Lawrence, USA

S. Duric, A. Ivanov, K. Kaadze, D. Kim, Y. Maravin, D.R. Mendis, T. Mitchell, A. Modak, A. Mohammadi

Kansas State University, Manhattan, USA

F. Rebassoo, D. Wright

Lawrence Livermore National Laboratory, Livermore, USA

E. Adams, A. Baden, O. Baron, A. Belloni, S.C. Eno, Y. Feng, N.J. Hadley, S. Jabeen, G.Y. Jeng, R.G. Kellogg, T. Koeth, A.C. Mignerey, S. Nabili, M. Seidel, A. Skuja, S.C. Tonwar, L. Wang, K. Wong

University of Maryland, College Park, USA

D. Abercrombie, B. Allen, R. Bi, S. Brandt, W. Busza, I.A. Cali, Y. Chen, M. D'Alfonso, G. Gomez Ceballos, M. Goncharov, P. Harris, D. Hsu, M. Hu, M. Klute, D. Kovalskyi, J. Krupa, Y.-J. Lee, P.D. Luckey, B. Maier, A.C. Marini, C. Mcginn, C. Mironov, S. Narayanan, X. Niu, C. Paus, D. Rankin, C. Roland, G. Roland, Z. Shi, G.S.F. Stephans, K. Sumorok, K. Tatar, D. Velicanu, J. Wang, T.W. Wang, Z. Wang, B. Wyslouch

Massachusetts Institute of Technology, Cambridge, USA

R.M. Chatterjee, A. Evans, S. Guts [†], P. Hansen, J. Hiltbrand, Sh. Jain, M. Krohn, Y. Kubota, Z. Lesko, J. Mans, M. Revering, R. Rusack, R. Saradhy, N. Schroeder, N. Strobbe, M.A. Wadud

University of Minnesota, Minneapolis, USA

J.G. Acosta, S. Oliveros

University of Mississippi, Oxford, USA

K. Bloom, S. Chauhan, D.R. Claes, C. Fangmeier, L. Finco, F. Golf, J.R. González Fernández, I. Kravchenko, J.E. Siado, G.R. Snow [†], B. Stieger, W. Tabb

University of Nebraska-Lincoln, Lincoln, USA

G. Agarwal, C. Harrington, L. Hay, I. Iashvili, A. Kharchilava, C. McLean, D. Nguyen, A. Parker, J. Pekkanen, S. Rappoccio, B. Roozbahani

State University of New York at Buffalo, Buffalo, USA

G. Alverson, E. Barberis, C. Freer, Y. Haddad, A. Hortiangtham, G. Madigan, B. Marzocchi, D.M. Morse, V. Nguyen, T. Orimoto, L. Skinnari, A. Tishelman-Charny, T. Wamorkar, B. Wang, A. Wisecarver, D. Wood

Northeastern University, Boston, USA

S. Bhattacharya, J. Bueghly, Z. Chen, A. Gilbert, T. Gunter, K.A. Hahn, N. Odell, M.H. Schmitt, K. Sung, M. Velasco

Northwestern University, Evanston, USA

R. Bucci, N. Dev, R. Goldouzian, M. Hildreth, K. Hurtado Anampa, C. Jessop, D.J. Karmgard, K. Lannon, W. Li, N. Loukas, N. Marinelli, I. Mcalister, F. Meng, K. Mohrman, Y. Musienko [44], R. Ruchti, P. Siddireddy, S. Taroni, M. Wayne, A. Wightman, M. Wolf, L. Zygala

University of Notre Dame, Notre Dame, USA

J. Alimena, B. Bylsma, B. Cardwell, L.S. Durkin, B. Francis, C. Hill, W. Ji, A. Lefeld, B.L. Winer, B.R. Yates

The Ohio State University, Columbus, USA

G. Dezoort, P. Elmer, B. Greenberg, N. Haubrich, S. Higginbotham, A. Kalogeropoulos, G. Kopp, S. Kwan, D. Lange, M.T. Lucchini, J. Luo, D. Marlow, K. Mei, I. Ojalvo, J. Olsen, C. Palmer, P. Piroué, D. Stickland, C. Tully

Princeton University, Princeton, USA

S. Malik, S. Norberg

University of Puerto Rico, Mayaguez, USA

V.E. Barnes, R. Chawla, S. Das, L. Gutay, M. Jones, A.W. Jung, B. Mahakud, G. Negro, N. Neumeister, C.C. Peng, S. Piperov, H. Qiu, J.F. Schulte, N. Trevisani, F. Wang, R. Xiao, W. Xie

Purdue University, West Lafayette, USA

T. Cheng, J. Dolen, N. Parashar, M. Stojanovic

Purdue University Northwest, Hammond, USA

A. Baty, S. Dildick, K.M. Ecklund, S. Freed, F.J.M. Geurts, M. Kilpatrick, A. Kumar, W. Li, B.P. Padley, R. Redjimi, J. Roberts [†], J. Rorie, W. Shi, A.G. Stahl Leiton, Z. Tu, A. Zhang

Rice University, Houston, USA

A. Bodek, P. de Barbaro, R. Demina, J.L. Dulemba, C. Fallon, T. Ferbel, M. Galanti, A. Garcia-Bellido, O. Hindrichs, A. Khukhunaishvili, E. Ranken, R. Taus

University of Rochester, Rochester, USA

B. Chiarito, J.P. Chou, A. Gandrakota, Y. Gershtein, E. Halkiadakis, A. Hart, M. Heindl, E. Hughes, S. Kaplan, O. Karacheban [23], I. Laflotte, A. Lath, R. Montalvo, K. Nash, M. Osherson, S. Salur, S. Schnetzer, S. Somalwar, R. Stone, S.A. Thayil, S. Thomas

Rutgers, The State University of New Jersey, Piscataway, USA

H. Acharya, A.G. Delannoy, S. Spanier

University of Tennessee, Knoxville, USA

O. Bouhali[88], M. Dalchenko, A. Delgado, R. Eusebi, J. Gilmore, T. Huang, T. Kamon[89], H. Kim, S. Luo, S. Malhotra, R. Mueller, D. Overton, L. Perniè, D. Rathjens, A. Safonov

Texas A&M University, College Station, USA

N. Akchurin, J. Damgov, V. Hegde, S. Kunori, K. Lamichhane, S.W. Lee, T. Mengke, S. Muthumuni, T. Peltola, S. Undleeb, I. Volobouev, Z. Wang, A. Whitbeck

Texas Tech University, Lubbock, USA

E. Appelt, S. Greene, A. Gurrola, R. Janjam, W. Johns, C. Maguire, A. Melo, H. Ni, K. Padeken, F. Romeo, P. Sheldon, S. Tuo, J. Velkovska, M. Verweij

Vanderbilt University, Nashville, USA

L. Ang, M.W. Arenton, B. Cox, G. Cummings, J. Hakala, R. Hirosky, M. Joyce, A. Ledovskoy, C. Neu, B. Tannenwald, Y. Wang, E. Wolfe, F. Xia

University of Virginia, Charlottesville, USA

P.E. Karchin, N. Poudyal, J. Sturdy, P. Thapa

Wayne State University, Detroit, USA

K. Black, T. Bose, J. Buchanan, C. Caillol, S. Dasu, I. De Bruyn, L. Dodd, C. Galloni, H. He, M. Herndon, A. Hervé, U. Hussain, A. Lanaro, A. Loeliger, R. Loveless, J. Madhusudanan Sreekala, A. Mallampalli, D. Pinna, T. Ruggles, A. Savin, V. Shang, V. Sharma, W.H. Smith, D. Teague, S. Trembath-reichert, W. Vetens

University of Wisconsin – Madison, Madison, WI, USA

[†]   Deceased.

[1]   Also at Vienna University of Technology, Vienna, Austria.

[2]   Also at Department of Basic and Applied Sciences, Faculty of Engineering, Arab Academy for Science, Technology and Maritime Transport, Alexandria, Egypt.

[3]   Also at Université Libre de Bruxelles, Bruxelles, Belgium.

[4]   Also at IRFU, CEA, Université Paris-Saclay, Gif-sur-Yvette, France.

[5]   Also at Universidade Estadual de Campinas, Campinas, Brazil.

[6]   Also at Federal University of Rio Grande do Sul, Porto Alegre, Brazil.

[7]   Also at UFMS, Nova Andradina, Brazil.

[8]   Also at Universidade Federal de Pelotas, Pelotas, Brazil.

[9]   Also at University of Chinese Academy of Sciences, Beijing, China.

[10]   Also at Institute for Theoretical and Experimental Physics named by A.I. Alikhanov of NRC 'Kurchatov Institute', Moscow, Russia.

[11]   Also at Joint Institute for Nuclear Research, Dubna, Russia.

[12]   Also at British University in Egypt, Cairo, Egypt.

[13]   Now at Ain Shams University, Cairo, Egypt.

[14]   Now at Fayoum University, El-Fayoum, Egypt.

[15]   Also at Purdue University, West Lafayette, USA.

[16]   Also at Université de Haute Alsace, Mulhouse, France.

[17]   Also at Tbilisi State University, Tbilisi, Georgia.

[18]   Also at Erzincan Binali Yildirim University, Erzincan, Turkey.

[19]   Also at CERN, European Organization for Nuclear Research, Geneva, Switzerland.

[20]   Also at RWTH Aachen University, III. Physikalisches Institut A, Aachen, Germany.

[21]   Also at University of Hamburg, Hamburg, Germany.

[22]   Also at Isfahan University of Technology, Isfahan, Iran, Isfahan, Iran.

[23]   Also at Brandenburg University of Technology, Cottbus, Germany.

[24]   Also at Skobeltsyn Institute of Nuclear Physics, Lomonosov Moscow State University, Moscow, Russia.

[25]   Also at Institute of Physics, University of Debrecen, Debrecen, Hungary, Debrecen, Hungary.

[26]   Also at Physics Department, Faculty of Science, Assiut University, Assiut, Egypt.

[27]   Also at Institute of Nuclear Research ATOMKI, Debrecen, Hungary.

[28]   Also at MTA-ELTE Lendület CMS Particle and Nuclear Physics Group, Eötvös Loránd University, Budapest, Hungary, Budapest, Hungary.

[29]   Also at IIT Bhubaneswar, Bhubaneswar, India, Bhubaneswar, India.

[30]   Also at Institute of Physics, Bhubaneswar, India.

[31]   Also at G.H.G. Khalsa College, Punjab, India.

[32] Also at Shoolini University, Solan, India.

[33] Also at University of Hyderabad, Hyderabad, India.

[34] Also at University of Visva-Bharati, Santiniketan, India.

[35] Also at Indian Institute of Technology (IIT), Mumbai, India.

[36] Also at Deutsches Elektronen-Synchrotron, Hamburg, Germany.

[37] Also at Department of Physics, University of Science and Technology of Mazandaran, Behshahr, Iran.

[38] Now at INFN Sezione di Bari ^{a}, Università di Bari ^{b}, Politecnico di Bari ^{c}, Bari, Italy.

[39] Also at Italian National Agency for New Technologies, Energy and Sustainable Economic Development, Bologna, Italy.

[40] Also at Centro Siciliano di Fisica Nucleare e di Struttura Della Materia, Catania, Italy.

[41] Also at Riga Technical University, Riga, Latvia, Riga, Latvia.

[42] Also at Consejo Nacional de Ciencia y Tecnología, Mexico City, Mexico.

[43] Also at Warsaw University of Technology, Institute of Electronic Systems, Warsaw, Poland.

[44] Also at Institute for Nuclear Research, Moscow, Russia.

[45] Now at National Research Nuclear University 'Moscow Engineering Physics Institute' (MEPhI), Moscow, Russia.

[46] Also at St. Petersburg State Polytechnical University, St. Petersburg, Russia.

[47] Also at University of Florida, Gainesville, USA.

[48] Also at Imperial College, London, United Kingdom.

[49] Also at P.N. Lebedev Physical Institute, Moscow, Russia.

[50] Also at California Institute of Technology, Pasadena, USA.

[51] Also at Budker Institute of Nuclear Physics, Novosibirsk, Russia.

[52] Also at Faculty of Physics, University of Belgrade, Belgrade, Serbia.

[53] Also at Università degli Studi di Siena, Siena, Italy.

[54] Also at Trincomalee Campus, Eastern University, Sri Lanka, Nilaveli, Sri Lanka.

[55] Also at INFN Sezione di Pavia ^{a}, Università di Pavia ^{b}, Pavia, Italy, Pavia, Italy.

[56] Also at National and Kapodistrian University of Athens, Athens, Greece.

[57] Also at Universität Zürich, Zurich, Switzerland.

[58] Also at Stefan Meyer Institute for Subatomic Physics, Vienna, Austria, Vienna, Austria.

[59] Also at Laboratoire d'Annecy-le-Vieux de Physique des Particules, IN2P3-CNRS, Annecy-le-Vieux, France.

[60] Also at Şırnak University, Sirnak, Turkey.

[61] Also at Department of Physics, Tsinghua University, Beijing, China, Beijing, China.

[62] Also at Near East University, Research Center of Experimental Health Science, Nicosia, Turkey.

[63] Also at Beykent University, Istanbul, Turkey, Istanbul, Turkey.

[64] Also at Istanbul Aydin University, Application and Research Center for Advanced Studies (App. & Res. Cent. for Advanced Studies), Istanbul, Turkey.

[65] Also at Mersin University, Mersin, Turkey.

[66] Also at Piri Reis University, Istanbul, Turkey.

[67] Also at Adiyaman University, Adiyaman, Turkey.

[68] Also at Ozyegin University, Istanbul, Turkey.

[69] Also at Izmir Institute of Technology, Izmir, Turkey.

[70] Also at Necmettin Erbakan University, Konya, Turkey.

[71] Also at Bozok Universitetesi Rektörlügü, Yozgat, Turkey.

[72] Also at Marmara University, Istanbul, Turkey.

[73] Also at Milli Savunma University, Istanbul, Turkey.

[74] Also at Kafkas University, Kars, Turkey.

[75] Also at Istanbul Bilgi University, Istanbul, Turkey.

[76] Also at Hacettepe University, Ankara, Turkey.

[77] Also at Vrije Universiteit Brussel, Brussel, Belgium.

[78] Also at School of Physics and Astronomy, University of Southampton, Southampton, United Kingdom.

[79] Also at IPPP Durham University, Durham, United Kingdom.

[80] Also at Monash University, Faculty of Science, Clayton, Australia.

[81] Also at Bethel University, St. Paul, Minneapolis, USA, St. Paul, USA.

[82] Also at Karamanoğlu Mehmetbey University, Karaman, Turkey.

[83] Also at Bingol University, Bingol, Turkey.

[84] Also at Georgian Technical University, Tbilisi, Georgia.

[85] Also at Sinop University, Sinop, Turkey.

[86] Also at Mimar Sinan University, Istanbul, Istanbul, Turkey.

[87] Also at Nanjing Normal University Department of Physics, Nanjing, China.

[88] Also at Texas A&M University at Qatar, Doha, Qatar.

[89] Also at Kyungpook National University, Daegu, Korea, Daegu, Republic of Korea.